HYDROGEOPHYSICS

Susan Hubbard

Lawrence Berkeley National Laboratory

1 Cyclotron Road, MS 90-1116

Berkeley, CA 94720

USA

sshubbard@lbl.gov

1-510-486-5266

Niklas Linde

Institute of Geophysics

University of Lausanne

Amphipôle – UNIL SORGE

CH-1015 Lausanne

niklas.linde@unil.ch

+41-21-692 44 01

Abstract

Developing a predictive understanding of subsurface flow and transport is complicated by the disparity of scales across which controlling hydrological properties and processes span. Conventional techniques for characterizing hydrogeological properties (such as pumping, slug, and flowmeter tests) typically rely on borehole access to the subsurface. Because their spatial extent is commonly limited to the vicinity near the wellbores, these methods often can not provide sufficient information to describe key controls on subsurface flow and transport. The field of hydrogeophysics has evolved in recent years to explore the potential that geophysical methods hold for improving the quantification of subsurface properties and processes relevant for hydrological investigations. This chapter is intended to familiarize hydrogeologists and water resource professionals with the state-of-the-art as well as existing challenges associated with hydrogeophysics. We provide a review of the key components of hydrogeophysical studies, which include: geophysical methods commonly used for shallow subsurface characterization; petrophysical relationships used to link the geophysical properties to hydrological properties and state variables; and estimation or inversion methods used to integrate hydrological and geophysical measurements in a consistent manner. We demonstrate the use of these different geophysical methods, petrophysical relationships, and estimation approaches through several field-scale case studies. Among other applications, the case studies illustrate the use of hydrogeophysical approaches to: quantify subsurface architecture that influence flow (such as hydrostratigraphy and preferential pathways); delineate anomalous subsurface fluid bodies (such as contaminant plumes); monitor hydrological processes (such as infiltration, freshwater-seawater interface dynamics, and flow through fractures); and estimate hydrological properties (such as hydraulic conductivity) and state variables (such as water content). The case studies

have been chosen to illustrate how hydrogeophysical approaches can yield insights about complex subsurface hydrological processes, provide input that improves flow and transport predictions, and provide quantitative information over field-relevant spatial scales. The chapter concludes by describing existing hydrogeophysical challenges and associated research needs. In particular, we identify the area of quantitative watershed hydrogeophysics as a frontier area, where significant effort is required to advance the estimation of hydrological properties and processes (and their uncertainties) over spatial scales relevant to the management of water resources and contaminants.

Keywords

Contaminant hydrology, data integration, environmental geophysics, flow and transport, geophysics, groundwater, hydraulic conductivity, hydrogeophysics, inversion, near-surface geophysics, permeability, petrophysical relationships, porosity, salinity, subsurface characterization, vadose zone, water content, water resources.

1. Introduction to Hydrogeophysics

The shallow subsurface of the earth is an extremely important geological zone, one that yields our water resources, supports our agriculture and ecosystems, influences our climate, and serves as the repository for our contaminants. The need to develop sustainable water resources for increasing population, agriculture, and energy needs and the threat of climate and land use change on ecosystems contribute to an urgency associated with improving our understanding of flow and transport processes in the shallow subsurface.

Developing a predictive understanding of subsurface flow and transport is complicated by the disparity of scales across which controlling hydrological properties and processes span (e.g., Gelhar, 1993). For example, the distributions of microfractures and geological formations both influence the hydraulic conductivity and thus subsurface flow, albeit over dramatically different spatial scales. Similarly, different hydrological processes may exert varying degrees of control on subsurface flow and transport as a function of the scale: the overall 'system response' of the particular problem may be dominated by seasonal precipitation patterns or by surface-groundwater interactions at the catchment scale; by the influence of groundwater pumping wells, gradients, and heterogeneity-induced mixing at the local scale; and by microbe-mineral interactions and diffusion at the grain scale (Figure 1). The level of subsurface characterization required for a particular problem depends therefore on many factors, including: the level of heterogeneity relative to the characterization objective, the spatial and temporal scales of interest, and regulatory or risk drivers. In some cases, reconnaissance efforts that delineate major characteristics of the study site may be sufficient while other investigations may require a much more intensive effort.

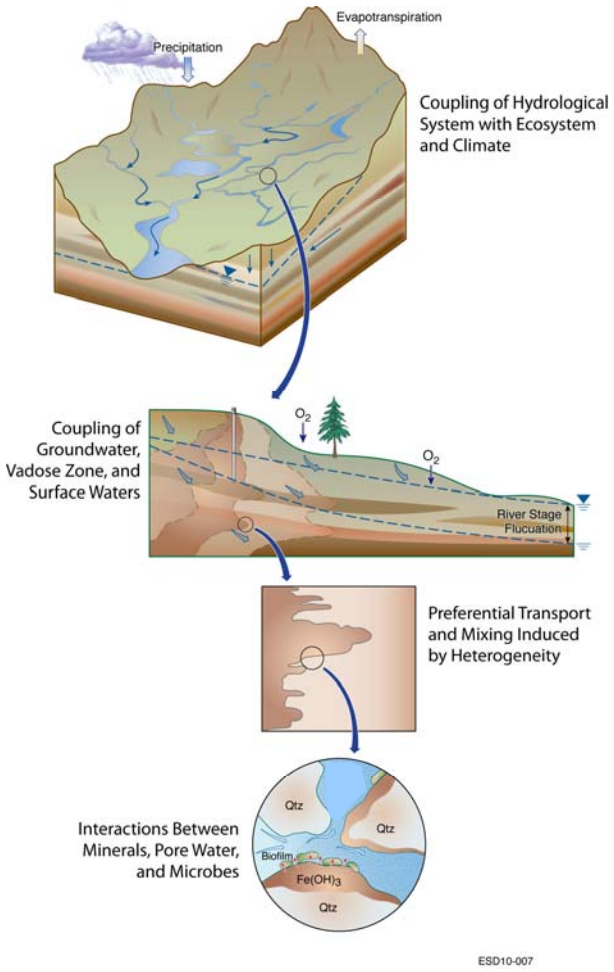

Figure 1 Subsurface flow and transport is impacted by coupled processes and properties that preferentially exert influence over a wide range of spatial scales, rendering characterization using borehole methods alone challenging.

Conventional techniques for characterizing or monitoring the hydrogeological properties that control flow and transport typically rely on borehole access to the subsurface. For example, established hydrological characterization methods (such as pumping, slug, and flowmeter tests) are commonly used to measure hydraulic conductivity in the vicinity of the wellbore (e.g.,

Freeze and Cherry, 1979; Butler, 2005; Molz et al., 1994), and wellbore fluid samples are often used for water quality assessment (e.g., Chapelle, 2001). Unfortunately, data obtained using borehole methods may not capture sufficient information away from the wellbore to describe the key controls on subsurface flow. The inability to characterize controlling properties at a high enough spatial resolution and over a large enough volume for understanding and predicting flow and transport processes using borehole methods often hinders our ability to predict and optimally manage associated resources.

The field of hydrogeophysics has developed in recent years to explore the potential that geophysical methods have for characterization of subsurface properties and processes relevant for hydrological investigations. Because geophysical data can be collected from many different platforms (such as from satellites and aircrafts, at the ground surface of the earth, and within and between wellbores), integration of geophysical data with direct hydrogeological or geochemical measurements can provide characterization information over a variety of spatial scales and resolutions. The main advantage of using geophysical data over conventional measurements is that geophysical methods can provide spatially extensive information about the subsurface in a minimally invasive manner at a comparatively high resolution. The greatest disadvantage is that the geophysical methods only provide indirect proxy information about subsurface hydrological properties or processes relevant to subsurface flow and transport.

Hydrogeophysical investigations strive to provide information that can be used to (1) develop insights about complex hydrological processes, (2) serve as input data to construct flow and transport models, and (3) guide the management of subsurface water resources and contaminants.

The field of hydrogeophysics builds on many decades of experience associated with the mining and petroleum industries, which have relied heavily on geophysical methods to guide the exploration of ore and hydrocarbons, respectively. Because geophysics has been used as a tool in these industries for so long, there is a relatively good understanding about methods and optimal data acquisition approaches for given problems, as well as about petrophysical relationships associated with the consolidated, high pressure, and high temperature subsurface environments common to those industries. However, such subsurface conditions are quite different from the shallow, low temperature, low pressure, and weakly consolidated environments that typify most hydrogeological investigation sites. The parameter values and the functional form of the petrophysical relationships that link geophysical properties to subsurface parameters, as well as the geophysical response itself, can vary dramatically between different types of environments.

In the last decade, many advances have been made that facilitate the use of geophysical data for shallow subsurface hydrogeological characterization. These advances include those associated with instrument development, interpretation procedures, petrophysical relationships relevant to near subsurface environments, integration or joint inversion approaches for combining multiple datasets, and coupled hydrological and geophysical modeling. Simultaneously, the number of publications related to hydrogeophysics has dramatically increased and are now common contributions to hydrological and geophysical journals such as *Water Resources Research*, *Journal of Hydrology*, *Vadose Zone Journal*, and *Geophysics*. Most hydrological and earth science professional meetings (such as American Geophysical Union, Geological Society of America, European Geosciences Union, etc.) now commonly host one or more hydrogeophysical special sessions at their annual meetings. These meetings have created an active environment

where geophysicists and hydrologists can interact to learn about each other's methods and challenges. Many ground-breaking hydrogeophysical studies have now been published by researchers with a formal hydrological training and it is becoming more common for geophysicists to strive to gain hydrological insights in addition to focusing primarily on advancing geophysical instrumentation and methodology. Some of the fairly recent hydrogeophysical advances are summarized in two edited books *Hydrogeophysics* (Rubin and Hubbard, 2005) and *Applied Hydrogeophysics* (Vereecken et al., 2006), as well as by numerous individual publications.

Generally, hydrogeophysical characterization and monitoring objectives can often be categorized into the following three categories:

1. Hydrological mapping of subsurface architecture or features (such as interfaces between key geological units, water table, or contaminant plume boundaries);
2. Estimating subsurface properties or state variables that influence flow and transport (such as hydraulic conductivity or soil moisture);
3. Monitoring subsurface processes associated with natural or engineered *in situ* perturbations (such as infiltration through the vadose zone and tracer migration).

There are several components that are common to most hydrogeophysical studies. First and foremost, it is critical to collect high-quality *geophysical datasets* using the geophysical method or methods that are most likely to provide data that can help to resolve the hydrogeological characterization or monitoring objective and that work well in the given environment. Although the corresponding geophysical properties (such as electrical conductivity/resistivity from

electrical and electromagnetic methods or dielectric constant from ground penetrating radar methods) can be used to infer hydrogeological properties or structures, *petrophysical relationships* must be developed and invoked at some stage to link the geophysical properties or data with the property or variable of interest (such as hydraulic conductivity or water content). *Integration or joint inversion methodologies* are used to systematically integrate or fuse disparate datasets (geophysical and hydrogeological) to obtain a meaningful interpretation that honors all data and physical laws. The ultimate step is the use of the integrated hydrogeophysical property or state model to interpret complex subsurface system processes or to guide the optimal management of subsurface water resources and contaminants.

The key objectives of this chapter are to familiarize hydrogeologists and water resource professionals with the state-of-the-art as well as the existing challenges associated with hydrogeophysics. We provide a review of the key components of many hydrogeophysical studies as well as example case studies that are relevant to understanding of hydrological behavior at the field scale. The remainder of this chapter is organized as follows. A brief description of some of the key geophysical methods that are used in hydrogeophysics is provided in Section 2. Descriptions of theoretical and empirical petrophysical relationships that can be used to link the geophysical attributes to the hydrogeological property of interest are discussed in Section 3. Section 4 reviews parameter estimation and integration methods that are used to combine disparate datasets for a consistent interpretation of critical flow and transport properties. Finally, in Section 5 we present various case studies that illustrate the use of geophysical datasets, petrophysics, and estimation methods to investigate near subsurface systems, with a particular

emphasis on case studies that are conducted over field scales relevant to water resources and contaminant remediation.

2. Geophysical Methods

The purpose of this section is to introduce some of the geophysical techniques that are most commonly used for hydrogeological studies, including: electrical resistivity tomography (ERT), induced polarization (IP), electromagnetic induction (EMI), self potential (SP), ground penetrating radar (GPR), seismic, surface nuclear magnetic resonance (SNMR), gravity, magnetics, and wellbore logging techniques. For each method, we provide a brief description of the underlying physical principles and instrumentation, common acquisition strategies, and general data reduction and interpretation methods. We restrict our discussions to practical use and limitations of common geophysical methods; geophysical theory (e.g., Telford et al., 1990) is beyond the scope of this discussion. For detailed information, references are given for each geophysical method. This discussion of classical geophysical methods is envisioned to compliment existing literature on what are typically considered to be hydrological sensors or measurement approaches, even though they rely on geophysical mechanisms; examples include soil moisture probes (time domain reflectometer and capacitance probes), electromagnetic wellbore flowmeters, and various remote sensing sensors deployed from air-borne or space-borne platforms. Reviews of these methods are provided by Vereecken et al. (2008) and Butler (2005). The discussion of geophysical methods provided here is augmented by Section 3, where several petrophysical relationships are provided that may permit the transfer of geophysical measurements into estimates of hydrological parameters.

2.1 Electrical Resistivity Method

For groundwater studies, electrical resistivity methods have perhaps been more frequently used than any other geophysical method. Resistivity is a measure of the ability to resist electrical current flow through materials; it is the inverse of electrical conductivity and is an intrinsic property of the material. In electrical resistivity methods, a typically low frequency (<1 Hz) current is injected into the ground between two current electrodes, while one or more pairs of potential electrodes are used to measure electrical potential differences. At the low frequencies measured, energy loss via ionic and electronic conduction dominates. Ionic conduction results from the electrolyte filling the interconnected pore space (Archie, 1942) as well as from surface conduction via the formation of an electrical double layer at the grain-fluid interface (e.g., Revil and Glover, 1997; Revil and Glover, 1998). Electronic conduction resulting from the formation of continuous conductive pathways by metallic minerals is typically not important for most environmental applications. The current distribution can be visualized by equipotential surfaces, with current flow lines running perpendicular to these surfaces. The fraction of total current flow that penetrates to a particular depth is a function of the current electrode spacing and location, the electrical resistivity distribution of the subsurface materials, and the topography.

Most resistivity surveys utilize a four-electrode measurement approach. To obtain a value for subsurface resistivity, two potential electrodes are placed at some distance from the current electrodes, and the difference in electrical potential or voltage is measured. This measurement, together with the injected current and the geometric factor which is a function of the particular electrode configuration and spacing, can be used to calculate resistivity for uniform subsurface conditions following Ohm's law. Common electrode configurations include the Wenner, the

Schlumberger, and the dipole-dipole arrays. In real heterogeneous (non-uniform) subsurface environments, the more general term “apparent resistivity” is used, which refers to the resistivity of an equivalent uniform media.

There are several modes of acquiring electrical data. *Profiling* is undertaken by moving the entire array laterally along the ground surface by a fixed distance after each reading to obtain apparent resistivity measurements over a relatively constant depth as a function of distance. As profiles give lateral variations in electrical conductivity but not information about vertical distribution, the interpretation of profile data is generally qualitative, and the primary value of the data is to delineate sharp lateral contrasts associated with vertical/near vertical contacts. *Vertical Electrical Sounding (VES)* curves give information about the vertical variations in electrical conductivity at a single ground surface location assuming an idealized one-dimensional resistivity structure. For example, soundings with the Wenner array are obtained by “expanding” the array along a straight line so that the spacing between the individual electrodes remains equal for each measurement, but increases after each measurement. The depth of investigation for a given measurement is a function of the electrode spacing as well as the subsurface resistivity contrasts; as the electrode spacing is increased, the data are increasingly sensitive to deeper structures.

Modern multi-channel geoelectrical equipment now includes multiplexing capabilities and automatic and autonomous computer acquisition, which greatly facilitate data acquisition within acceptable timeframes. Such surface imaging, now commonly called *electrical resistivity tomography or ERT,* allows the electrodes (tens to hundreds) to be used alternatively as both current and potential electrodes to obtain two- or three-dimensional electrical resistivity models

(e.g., Günther et al., 2006). In fact, when performing ERT, it is limiting to restrict the measurement sequence to a given configuration type, since optimal data sets often consist of a combination of traditional and non-traditional configuration types (Stummer et al., 2004; Wilkinson et al., 2006). With the development of advanced and automated acquisition systems, robust inversion routines, and the capability of recording tens of thousands of measurements per hour, ERT has proven to be useful for dynamic process monitoring using electrodes placed at the ground surface or in wellbores. A review of surface and crosshole ERT methods for hydrogeological applications is given by Binley and Kemna (2005), and discussion of petrophysical relationships that link the electrical properties with hydrological properties of interest is described in Section 3.1.

2.2 Induced Polarization (IP) Methods

Induced polarization (IP) methods measure both the resistive and capacitive properties of subsurface materials. IP measurements can be acquired using the same four-electrode geometry that is conventionally used for electrical resistivity surveys, although IP surveys typically employ non-polarizing electrodes. Surveys can be conducted in the time domain as well as in the frequency domain. In the time-domain, the current is injected and the decay of the voltage over time is measured. Frequency-domain methods measure the impedance magnitude and phase shift of the voltage relative to an injected alternating current. Spectral Induced Polarization (SIP) methods measure the polarization relaxation over many frequencies (typically over the range of 0.1-1000 Hz). The voltage decay (in the time-domain) and spectral response (in the frequency domain) is caused by polarization of ions in the electrical double layer at the mineral-fluid interface, by accumulation of electrical charges at pore space constrictions (e.g., pore-throats),

and by conduction in the pore fluid and along the fluid-grain boundaries. More information about IP methods is provided by Binley and Kemna (2005) and Leroy and Revil (2009).

The linkage between induced polarization attributes, granulometric properties, and interfacial phenomena suggests that it also holds significant potential for exploring hydrogeological variabilities (e.g., Slater and Lesmes, 2002) as well as complex biogeochemical processes associated with contaminant remediation (e.g., Williams et al., 2005, 2009; Slater et al., 2007). Section 3.3 provides discussion of petrophysical models associated with SIP datasets.

2.3 Self Potential (SP) Methods

SP is a passive method where naturally occurring electric fields (voltage gradients) are measured at the ground surface or in wellbores using non-polarizable electrodes and a high impedance voltmeter. Electrical potentials measured with the SP method obey a Poisson's equation with a source term given by the divergence of an electrical source current density (e.g., Minsley et al., 2007). The source current density has several possible contributors, including those associated with ground water flow, redox phenomena, and electro-diffusion. The electrokinetic contribution associated with the flow of ground water in a porous medium (or more precisely, with the drag of charges contained in the diffuse layer that surrounds mineral surfaces) has been recognized for many decades and has been used to qualitatively interpret SP signals in terms of seepage beneath dams or to map groundwater flow (e.g., Poldini, 1938). However, only more recently have such datasets been used to quantify hydrological properties by coupling equations that represent volumetric fluid flux and volume current density, which are linked by a coupling coefficient (e.g., Sill, 1983; Revil et al., 2003). The underlying physics of the redox and electro-diffusion contributions are now better understood and current research is advancing our ability to use SP

for quantitative hydrogeochemical characterization (such as for characterizing field-scale redox gradients; refer to case study provided in Section 5.2).

The SP method is the only geophysical method that is directly sensitive to hydrological fluxes (e.g., Sill, 1983). Even if several alternative formulations exist to describe electrokinetic phenomena, we consider here the case where the self-potential sources are expressed in terms of Q_v, where Q_v is expressed as excess charge in the diffuse double layer per saturated pore volume. The relative movement of an electrolyte with respect to mineral grains with a charged surface area results in so-called streaming currents (e.g., Sill, 1983). These currents are intimately linked to the Darcy velocity **U** and an effective excess charge Q_v^{eff} along the hydrological flow paths. A practical formulation of the streaming currents that corresponds to this parameterization is (e.g., Revil and Linde, 2006)

$$J_s = Q_v \mathbf{U} \tag{1}$$

This equation is only strictly valid when the size of the double-layer is comparable to the size of the pores (see Revil and Linde (2006) for a description of chemico-electromechanical coupling under such conditions) and when internal permeability variations within the averaged volume are small. Equation 1 can be used in heterogeneous media or in coarse sediments when we replace Q_v with an effective Q_v^{eff} that is scaled with the relative contributions to permeability of all flow paths in the media (Linde, 2009). It is straightforward to deduce Q_v^{eff} of aquifer materials in the laboratory using the relationship (Revil and Leroy, 2004)

$$C_{sat} = \frac{Q_v^{eff} k}{\mu_w \sigma}, \tag{2}$$

where k is the permeability and μ_w is the dynamic water viscosity. The voltage coupling C_{sat} can be obtained using a simple experimental setup, for example, using the type of column experiment presented by Suski et al. (2006).

The dependence of $Q_{v,sat}^{eff}$ with water content depends on the geological media considered, but it is to a first order inversely related to water content (Linde et al., 2007; Linde, 2009). The source current that is responsible for observed electrical potential signals associated with these processes is given by the divergence of equation 1 (e.g., Linde et al., 2007).

2.4 Controlled Source Inductive Electromagnetic (EM) Methods

Controlled-source inductive EM methods use a transmitter to pass a time- or frequency varying current through a coil or dipole placed on the earth's surface, in boreholes, mounted on an aircraft or towed behind a ship. Governed by Maxwell's equations and typically operating in the 1-15 kHz range, this alternating current produces a time-varying primary magnetic field, which in turn interacts with the conductive subsurface to induce time-varying eddy currents. These eddy currents give rise to a secondary EM field. Attributes of this secondary magnetic field, such as amplitude, orientation, and/or phase shift, can be measured by a receiver coil. By comparing these attributes with those of the primary field, information about the presence of subsurface electrical conductors or the subsurface electrical conductivity distribution can be inferred. Because a conductive subsurface environment or target is required to set up the secondary field measured with inductive EM methods, EM methods are best suited for use when attempting to detect the presence of high-conductivity subsurface targets, such as salt water saturated sediments or clay layers. However, because coils do not require contact with the ground, EM

methods are often more successful on electrically resistive or paved ground than the classical DC resistivity method, which requires electrode contact.

As with ERT and SIP data, EM induction data can be collected in profile or sounding mode. The mode of acquisition and the resolution and depth penetration of the data are dictated by the electrical conductivity distribution of the subsurface and the coil spacing and source configuration. For frequency domain systems, high transmitter frequencies permit high-resolution investigation of subsurface conductors at shallow depths while lower transmitter frequencies permit deeper observations but at a loss in resolution. Time domain systems measure the secondary magnetic field as a function of time, and early-time measurements yield information about the near-surface, while later-time measurements are increasingly influenced by the electrical properties at larger depths. The depth of penetration and resolution are also governed by coil configuration; the measurements from larger coil separations are influenced by electrical properties at greater depths, while smaller coil spacings sample from the near-surface. A review and discussion of the use of controlled source EM methods for hydrogeological investigations is given by Everett and Meju (2005). It should be noted that it is also possible to use civilian and military radio transmitters, operating in the 10-250 kHz frequency range, as the source signal. These are the signals used in the popular very low frequency (VLF) (e.g., Pedersen et al., 1994) and radio magnetotelluric (RMT) (e.g., Linde and Pedersen, 2004) techniques.

2.5 Ground Penetrating Radar (GPR) Methods

GPR methods use electromagnetic energy at frequencies of ~10 MHz to 1GHz to probe the subsurface. At these frequencies, the separation (polarization) of opposite electric charges within a material that has been subjected to an external electric field dominates the electrical response.

GPR systems consist of an impulse generator which repeatedly sends a particular voltage and frequency source to a transmitting antenna. When the source antenna is placed on or above the ground surface, spherical waves are radiated downward into the soil. In general, GPR performs better in unsaturated coarse or moderately coarse textured soils; GPR signal strength is strongly attenuated in electrically conductive environments (such as systems dominated by the presence of clays or high ionic strength pore fluids). Together, the electrical properties of the host material and the frequency of the GPR signal primarily control the resolution and the depth of penetration of the signal. Increasing the frequency increases the resolution but decreases the depth of penetration.

GPR datasets can be collected in the time- or in the frequency-domain. Time-domain systems are most commonly used in near-surface investigations. Generally, one chooses a radar center frequency that yields both sufficient penetration and resolution; for field applications this is often between 50 to 250 MHZ. However, significant advances have been made in the development of frequency domain systems. Lambot et al. (2004a) describe a stepped-frequency continuous-wave radar deployed using an off-ground horn antenna over the frequency range of 0.8-3.4 GHz. The wide bandwidth and off-ground configuration permits more accurate modeling of the radar signal, thus potentially leading to improved estimates of subsurface parameters (Lambot et al., 2004b, 2006).

The most common ground surface GPR acquisition mode is surface common-offset reflection, in which one (stacked) trace is collected from a transmitter-receiver antenna pair pulled along the ground surface. With this acquisition mode, GPR antennas can be pulled along or above the

ground surface at walking speed. When the electromagnetic waves in the ground reach a contrast in dielectric constants, part of the energy is reflected and part is transmitted deeper into the ground. The reflected energy is displayed as two-dimensional profiles that indicate the travel time and amplitude of the reflected arrivals; such profiles can be displayed in real time during data collection and can be stored digitally for subsequent data processing. An example of the use of GPR profiles for interpreting subsurface stratigraphy is provided in Section 5.1.

The velocity of the GPR signal can be obtained by measuring the travel time of the signal over a known distance between the transmitter and the receiver. The propagation phase velocity (V) and signal attenuation are controlled by the dielectric constant (κ) and the electrical conductivity of the subsurface material through which the wave travels. At the high frequency range used in GPR, the velocity in a low electrical conductivity material can be related to the dielectric constant, also known as the dielectric permittivity, as (Davis and Annan, 1989):

$$\kappa \approx \left(\frac{c}{V}\right)^2, \tag{3}$$

where c is the propagation velocity of electromagnetic waves in free space (3×10^8 m/s).

Approaches that facilitate electromagnetic velocity analysis include surface common-midpoint (CMP), crosshole tomography acquisition, as well as analysis of the groundwave arrival recorded using common-offset geometries. Full-waveform inversion approaches have been recently developed (e.g., Ernst et al., 2007; Sassen and Everett, 2009) that offer potential for improved subsurface property characterization over methods based on travel times alone. Discussion of petrophysical relationships that link dielectric permittivity with hydrological properties of

interest is described in Section 3.2. A review of GPR methods applied to hydrogeological applications is given by Annan (2005).

2.6 Seismic Methods

Seismic methods common to hydrological investigations use high-frequency (~100 to 5000 Hz) pulses of acoustic energy to probe the subsurface. These pulses are generally artificially produced (using weight drop, hammers, explosives, piezoelectric transducers, etc.) and propagate outward as a series of wavefronts. The passage of the wavefront creates a motion that can be detected by a sensitive geophone or hydrophone. According to the theory of elasticity upon which seismic wave propagation is based, several different waves are produced by a disturbance; these waves travel with different propagation velocities that are governed by the elastic constants and density of the material. The P-wave energy is transmitted by a back-and-forth particle movement in the direction of the propagating wave. Transverse waves, also called S (secondary or shear)-waves, have lower velocities than the P-wave and thus arrive later in the recording. P-wave arrivals are the easiest to detect and most commonly used arrival; we focus here exclusively on information available from P-waves. The principles of seismic reflection, refraction, and tomographic methods are briefly described below.

The surface reflection technique is based on the return of reflected P-waves from boundaries where velocity and density (or seismic impedance) contrasts exist. Processing of seismic reflection data generally produces a wiggle-trace profile that resembles a geologic cross section. However, due to the lack of well-defined velocity contrasts and strong signal interference in shallow unconsolidated and unsaturated materials, seismic reflection approaches to image near

subsurface architecture can be challenging. With refraction methods, the incident ray is refracted along the target boundary before returning to the surface. The refracted energy arrival times are displayed as a function of distance from the source, and interpretation of this energy can be accomplished by using simple software or forward modeling techniques. As with GPR methods, the arrival times and distances can be used to obtain velocity information directly. More advanced applications include multi-dimensional inversion for the subsurface velocity distribution using many first arrival travel-times corresponding to refracted energy for many combinations of transmitter and receiver locations. Refraction techniques are most appropriate when there are only a few shallow (<50m) targets of interest, or where one is interested in identifying gross lateral velocity variations or changes in interface dip. Seismic refraction methods yield much lower resolution than seismic reflection and crosshole methods. However, because refraction methods are inexpensive and acquisition may be more successful in unsaturated and unconsolidated environments, they are often chosen over reflection methods for applications such as determining the depth to the water table and to the top of bedrock, the gross velocity structure, or for locating significant faults. With crosshole seismic tomographic data, the multiple sampling of the inter-wellbore area via raypaths that emanate from instruments lowered down boreholes permits very detailed estimation of the velocity structure that can be used to estimate hydrogeological properties. A review of shallow seismic acquisition and processing techniques is given by Steeples (2005).

2.7 Surface Nuclear Magnetic Resonance

Surface Nuclear Magnetic Resonance (SNMR) is a geophysical method that takes advantage of the NMR response of hydrogen protons, which are components of water molecules, to estimate

water content. This method involves the use of a transmitting and a receiving loop to induce and record responses to an electromagnetic excitation induced at the resonance frequency of protons (the Larmor frequency). Under equilibrium conditions, the protons of water molecule hydrogen atoms have a magnetic moment that is aligned with the earth's local magnetic field. Upon excitation, the axis of the precession is modified. When the external field is removed, relaxation occurs as a function of the spatial distribution, amount, and mobility of water; this relaxation manifest itself as an electromagnetic signal that decays over time. Through use and analysis of different excitation intensities, initial amplitudes and decay time, approaches have been proposed to estimate the density distribution of hydrogen atoms as well as associated pore and grain size and water content.

Although SNMR holds significant potential for directly investigating subsurface hydrological properties, it is still in an early stage of development and its resolving power is rather limited. As described by Yaramanci et al. (2005), advances are needed to overcome induction effects and inversion errors associated with multi-dimensional heterogeneities and regularization. A further problem with this method is that it is very sensitive to cultural EM noise and that the measured signals are often weak. Hertrich (2008) provides a review of SNMR for groundwater applications, and describes recent algorithm and method development.

2.8 Gravity

Measurements of changes in gravitational acceleration can be used to obtain information about subsurface density variations that can in turn be related to variations in lithology or moisture content. The common measuring device for this potential field method is a gravimeter, an

instrument which is portable and easy to use. An extremely sensitive spring balance inside the gravimeter measures differences in the weight of a small internal object from location to location; the weight differences are attributed to changes in the acceleration of gravity due to lateral variations in subsurface density. Measurements can be collected at a regional or local scale depending on the station spacing, which is usually less than half of the depth of interest.

The theoretical response to the gravitational field due to such factors as the datum, latitude, terrain, drift, and regional gradient are typically compensated for prior to interpretation of the remaining gravity anomaly. Qualitative interpretation usually consists of constraining a profile or contoured anomaly map with other known geologic information to delineate, for example, the boundary of a sedimentary basin that overlies denser bedrock. A general review of the gravity technique and applications to environmental studies is given by Hinze (1990). More recently, microgravity studies have recently been performed in an attempt to quantify changes in water storage associated with hydrological processes (e.g., Krause et al., 2009) and to characterize cavities in karstic terrains (Styles et al., 2005).

2.9 Magnetics

Magnetic methods obtain information related to the direction, gradient, or intensity of the earth's magnetic field. The intensity of the magnetic field at the earth's surface is a function of the location of the observation point in the primary earth magnetic field as well as from contributions from local or regional variations of magnetic material such as magnetite, the most common magnetic mineral. After correcting for the effects of the earth's natural magnetic field, magnetic data can be presented as total intensity, relative intensity, and vertical or horizontal gradient

anomaly profiles or contour maps. Interpretation of magnetic surveys generally involves forward modeling or mapping of the anomalies and correlating them with other known geologic information. As magnetic signatures depend to a large extent on magnetic mineral content, which is low in most sediments that comprise aquifers, magnetics is not commonly employed for hydrological investigations, but it can be a very powerful technique to locate lateral boundaries of landfills. Exceptions include mapping subsurface structures (basement topography, faults, paleochannels), provided that a sufficient magnetic signature or contrast exists. A review of magnetic methods as applied to environmental problems is given by Hinze (1990).

2.10 Well Logging

Well logging refers to the process of recording and analyzing measurements collected discretely or continually within wellbores. Borehole measurements are made by lowering a probe into the borehole on the end of an electric cable. The probe, generally 2.5 to 10.0 cm in diameter and 0.5 to 10.0 m in length, typically encloses sources, sensors, and the electronics necessary for transmitting and recording signals. A variety of different types of wellbore probes are available; perhaps the most common for hydrological studies include: SP, electrical, electromagnetic, gamma-gamma, natural gamma, acoustic, temperature, flowmeter, neutron-neutron, televiewer and caliper logs. The volume of investigation of the borehole measurement is related to the log type, source-detector spacing, the borehole design, and the subsurface material. The well log measurements can be compared with each other and with direct measurements (such as from core samples) to develop site specific petrophysical relationships. Log data are also useful to ‘tie’ hydrological and geological data collected at the wellbore location with geophysical signatures of property variations collected using surface or crosshole geophysical data. References for

borehole geophysics applied to hydrogeologic investigations are given by Keys (1989) and Kobr et al. (2005).

3. Petrophysical Models

To be useful in hydrology, geophysical data and hence the corresponding geophysical properties need to be sensitive to hydrological primary (e.g., total and effective porosity, permeability) or state variables (e.g., salinity, water content, pressure gradients). In this section, we introduce different petrophysical models that link hydrological and geophysical properties. We focus on models related to electrical properties, since they dominate hydrogeophysical applications through methods such as ERT, SIP, EM and GPR (see Section 2). Pertinent models related to gravity, seismics, and borehole geophysical data are not considered here for brevity, but can be found in references such as Mavko et al. (1998), Schön et al. (1996), Guéguen and Palciauskas (1994), and Carcione et al. (2007). A wealth of models for electrical properties in porous media has been proposed and only main results are summarized below; the reader is referred to Lesmes and Friedman (2005), Keller (1987), and Slater (2007) for more information. The petrophysical models discussed below were chosen because they are fairly general, but also because most of them share a similar parameterization.

Purely mathematical models are useful to define bounds on properties, such as the classical Hashin-Shtrikman bounds (Hashin and Shtrikman, 1962). More common in hydrogeophysical studies are the use of semi-empirical models that partly incorporate geometrical and physical properties of the components that comprise the porous media. Examples of such models are Archie's law (Archie, 1942) or the complex refractive index model (Birchak et al., 1974). In

many cases, purely empirical relationships are obtained by fitting polynomial functions (e.g., Topp et al., 1980). Below, we briefly review petrophysical models associated with electrical conductivity, dielectric permittivity, complex conductivity, and electrokinetics.

3.1 Electrical Conductivity

The conductive and capacitive properties of an isotropic and homogeneous media can be represented by a complex conductivity (σ^*), a complex resistivity (ρ^*), or a complex permittivity (ε^*)

$$\sigma^*(\omega) = \frac{1}{\rho^*(\omega)} = i\omega\varepsilon^*(\omega), \tag{4}$$

where ω is the angular frequency and $i = \sqrt{-1}$. It is common practice to refer to the real valued component of $\sigma^*(\omega) = \sigma'(\omega) + i\sigma''(\omega)$ at low frequencies (say 0-250 kHz) as σ and the real valued relative permittivity at high frequencies (10-1000 MHz) as $\kappa = \varepsilon'/\varepsilon_0$, where ε' is the effective permittivity of the media and ε_0 is the permittivity of vacuum. It is important to note that in these frequency ranges both properties, σ and κ, have a weak frequency dependency (e.g., see Figure 4.1 in Lesmes and Friedman (2005)) that needs to be taken into account for quantitative comparisons. Low-frequency polarization $\sigma''(\omega)$ is discussed in Section 3.3

Archie's law

The aggregated empirical Archie's first and second law (Archie, 1942), expressed here in terms of electrical conductivity, is probably the most commonly used model to interpret electrical conductivity in hydrological studies

$$\sigma = \sigma_w S_w^n \phi^m = \sigma_w S_w^n F^{-1}, \tag{5}$$

where σ is the bulk electrical conductivity of the media, σ_w is the electrical conductivity of the pore fluid, S_w is the water saturation, n is the water saturation exponent, ϕ is the porosity, and m is the cementation exponent. The electrical formation factor F is defined in the absence of surface conductivity σ_s as (e.g., Revil et al., 1998)

$$\frac{1}{F} \equiv \lim_{\sigma_s \to 0} \left(\frac{\sigma}{\sigma_w} \right) = \phi^m. \tag{6}$$

The attraction of Archie's law in hydrological applications is obvious since it includes key properties, namely the electrical conductivity of the pore fluid related to salinity and the inverse of the electrical formation factor, which can be thought of as an effective interconnected porosity (Revil and Cathles, 1999). Archie's law not only explains a lot of experimental data, but is physically justified when surface conduction is negligible (Sen et al., 1981). In the vadose zone, the water saturation exponent may display significant hysteresis (Knight, 1991). Archie's law is only valid for a continuous water phase, which might break down in dry areas where evaporation is significant (e.g., Shokri et al., 2009). Another more serious problem with this model is that surface conduction, which plays a role when significant clay and silt fractions are present in the media, is ignored.

Waxman-Smits law

A number of models have been proposed to incorporate surface conduction. One of the most commonly used models that includes surface conduction in saturated media is the model of Waxman and Smits (1968)

$$\sigma = \frac{1}{F}\left(\sigma_w + BQ_v\right), \tag{7}$$

where B is the equivalent conductance per ion and Q_v is the density of counter ions per unit pore volume. Electrical conduction is here modeled as being composed of an electrical path in the pore volume and another parallel path at the mineral-water interface. This equation has been extensively used in the oil industry and it provides normally a good fit to experimental data when the electrolytic conductivity term dominates over the surface conductivity term (e.g., Waxman and Smits, 1968; Johnson et al., 1986; Sen et al., 1988). One problem with Waxman and Smits' model is that it uses an average Q_v determined by titration while only the excess charge located along the conducting paths in the pore space will contribute to electrical flow. Another problem arises when surface conductivity becomes more important, since the electrical conduction paths change and can no longer be expressed by F (see Equation 5) only (Johnson et al., 1986; Revil et al., 1998).

The Johnson, Koplik and Schwarz model

A fundamental length-scale parameter Λ was introduced by Johnson et al. (1986) as

$$\frac{2}{\Lambda} = \frac{\int \left|\nabla \psi_0(\mathbf{r})\right|^2 dS}{\int \left|\nabla \psi_0(\mathbf{r})\right|^2 dV_p}, \tag{8}$$

where $\nabla \psi_0(\mathbf{r})$ is the electrical potential gradient at position $\mathbf{r}$ in the absence of surface conductivity from a current source imposed from the sides and where the integration is performed over the mineral-water interface (S) and the pore volume (V_p), respectively. It follows that $2/\Lambda$ is an effective surface-to-pore-volume ratio weighted by the local strength of the electric field. This weighting eliminates contributions from dead-end pores (Johnson et al., 1986). Johnson et al. (1986) use a perturbation technique to derive the following equation

$$\sigma = \frac{1}{F}\left(\sigma_w + \frac{2\Sigma_s}{\Lambda} \right) + O\left(\Sigma_s^2\right), \tag{9}$$

where the specific surface conductivity is given by (e.g., Schwartz et al., 1989)

$$\Sigma_s = \int_0^\infty \left[\sigma(\varepsilon) - \sigma_w \right] d\varepsilon, \tag{10}$$

where ε measures the distance along a normal directed into the pore space from the grain boundary. The contributions to $\sum_s$ become insignificant for values much larger than the Debye screening length that is at most some 100 Å. The $\sum_s$ is fairly well-known and is much less variable than Λ (Leroy and Revil, 2004).

Neglecting second-order terms in equation 9, $O\left(\Sigma_s^2\right)$, is only valid in the vicinity of the high-salinity limit. Schwarz et al. (1989) extended the theory of Johnson et al. (1986) to the low-salinity limit in which the electrical flow paths are determined by regions with significant surface conduction. They showed that Padé approximants (a ratio of two polynomials) are effective to interpolate between the high- and low salinity limits.

Johnson et al. (1986) also show that Λ can be used to predict permeability k with a high predictive power using the relation (see also Bernabé and Revil (1995))

$$k \approx \frac{\Lambda^2}{4F}. \tag{11}$$

Self-similar models

Another approach to model electrical conductivity is based on self-similar models with electrolytic conduction only (Sen et al., 1981) or with surface conductivity included (Bussian,

1983). Revil et al. (1998) extended the model of Bussian (1983) to explicitly model the different conduction paths taken by anions and cations. Tortuosity affecting the migration of the anions is given by $F\phi$, but the dominant conduction paths for the cations shift toward the conduction paths defined by the distribution of Q_v at the mineral-water interfaces as the salinity decreases.

The ubiquitous presence of surface conductivity in geological porous media make models of electrical conductivity alone uncertain tools in hydrological studies, since a moderately high electrical conductivity can be explained by either a fairly high σ_w with a well-connected pore space (i.e., low F) without any clay particles, or a low σ_w and a poorly connected pore space (i.e., high F) with a moderate clay fraction. The hydrological behaviors of these two types of media are fundamentally different and electrical conductivity data alone may not offer even qualitative information about the dominant hydrological properties (e.g., Purvance and Andricevic, 2000). To make quantitative predictions, it is therefore often needed to have access to other types of geophysical (such as IP) or geological data or to perform time-lapse experiments, where temporal variations in the geophysical data are recorded (e.g., Binley et al., 2002a).

3.2 Dielectric Permittivity

Volume-averaging

Electrical polarization at the frequencies used in ground-penetrating radar GPR (10-1000 MHz) is mainly determined by water content and less by mineralogy, even if polarizations of mineral grains need to be considered. Due to the need of complimentary data in most hydrogeophysical applications, it is common to use estimates of both electrical conductivity and the relative permittivity (e.g., Binley et al., 2002a; Linde et al., 2006a). When explaining relative permittivity

data it can therefore be useful to use a relative permittivity model that shares a similar parameterization of the pore geometry as the one used to explain electrical conductivity. Such an approach was presented by Pride (1994) who used a volume averaging approach to derive the following equation for relative permittivity

$$\kappa = \left[\frac{1}{F}\left(\kappa_w - \kappa_s\right) + \kappa_s \right], \tag{12}$$

where κ_w is the relative permittivity of water ($\kappa_w \approx 80$) and κ_s is the relative permittivity of the solid (κ_s=3-8). This equation was extended by Linde et al. (2006a) to incorporate partial saturations as

$$\kappa = \frac{1}{F}\left[S_w^n \kappa_w + \left(1 - S_w^n\right)\kappa_a + \left(F - 1\right)\kappa_s \right], \tag{13}$$

where κ_a is the relative permittivity of air (κ_a =1). See Linde et al. (2006a) for a corresponding model for electrical conductivity with surface conductivity included.

One of the most common petrophysical models used to estimate water content from relative permittivity data is the so-called Lichteneker-Rother model (e.g., Guéguen and Palciauskas, 1994)

$$\kappa^a = \sum_{i=1}^{n} \phi_i \kappa_i^{\alpha}, \tag{14}$$

where the subscript *i* indicates the contribution of each phase (e.g., rock matrix, water, and air). Equation (14) with α=0.5 is referred to as the complex refractive index model (Birchak et al., 1974)

$$\sqrt{\kappa} = \theta\sqrt{\kappa_w} + \left(\phi - \theta\right)\sqrt{\kappa_a} + \left(1 - \phi\right)\sqrt{\kappa_s}, \tag{15}$$

where θ is water content. Brovelli and Cassiani (2008) showed that this commonly used model is only valid when the cementation exponent *m* is close to 2 and when the dielectric contrast between phases are large. This means that Equation (15) is based on an implicit assumption about the connectedness of the pore space that in reality varies (e.g., *m* is typically around 1.5 in unconsolidated aquifer materials; Lesmes and Friedman, 2005). Recently, Brovelli and Cassiani (2010) showed convincingly that an appropriately weighted combination of the lower- and upper Hashin-Shtrikman bounds using the cementation factor could predict permittivity measurements very well.

Topp's equations

A set of models that are purely empirical but have high predictive power in soils are the so-called Topp's equations that were derived at high frequencies for different soil types. The general Topp equation (Topp et al., 1980) when the soil type is unknown is

$$\kappa = 3.03 + 9.3\theta + 146\theta^2 - 76.7\theta^3. \quad (16)$$

3.3 Complex Conductivity

Cole-Cole model

We now focus on the frequency behavior of the imaginary component of the complex electrical conductivity (Equation 4) $\sigma''(\omega)$ at low frequencies. Recent experiments suggests that the electrochemical polarization of a grain is dominated by the mineral/water interface of the Stern layer and Maxwell-Wagner effects associated with accumulation of electrical charges at pore throats (Leroy et al., 2008). SIP data (also referred to as complex conductivity, Kemna, et al., 2000) have been identified as the most promising method to develop robust inferences of

polarization processes (Ghorbani et al., 2007) and potentially permeability in hydrological studies (Slater and Lesmes, 2002; Binley et al., 2005). The most common petrophysical model used in SIP is the phenomenological Cole-Cole model (Cole and Cole, 1941) or combinations of several Cole-Cole models. The Cole-Cole model can be expressed as

$$\sigma^*(\omega) = \sigma_0 \left[1 + m \left(\frac{(i\omega\tau)^c}{1 + (i\omega\tau)^c (1-m)} \right) \right], \quad (17)$$

where σ_0 is the conductivity at the direct-current limit, τ is the mean relaxation time, c is an exponent that typically takes values in the range of 0.1-0.6, and m is the chargeability (m=1-σ_0/σ_∞, where σ_∞ is the electrical conductivity at high frequency). Parameters of this model might be sensitive to specific surface area (Börner and Schön, 1991; Slater et al., 2006), dominant pore-throat sizes (Scott and Barker, 2003) or effective grain sizes (Slater and Lesmes, 2002). Laboratory measurements on sandstone suggest a strong correlation between the relaxation time and the permeability (r^2=0.78) (Binley et al., 2005) and promising results have been reported from field applications (Hördt et al., 2007). It is likely that new physical models based on a more physical parameterization of the pore space that is consistent with the ones developed for other electrical properties (e.g., Leroy et al., 2008; Leroy and Revil, 2009) will help to gain a better understanding of the low-frequency polarization response and its sensitivity to hydrological parameters. In particular, it is important to develop a theory that holds at any frequency and that take the characteristics of the electrical double layer and the surface chemistry into account.

4. Parameter Estimation/Integration Methods

This section addresses how geophysical data and models can be used together with hydrological data and models to improve the imaging of hydrological properties or monitoring of hydrological

processes. The approaches that have been presented in the literature differ mainly in how they represent the model parameter space; what importance and representation is given to a priori information; at what stage different data types are coupled; how uncertainties in the observations, the forward models, and the petrophysical models are treated. Figure 2 provides a schematic view of how geophysical and hydrological data and models can be integrated at different stages in the inversion process. The figure can also be seen as a general representation of how joint inversion can be carried out for the case of two data types. For an in-depth treatment of inversion theory, we refer to Menke (1984), Parker (1994), McLaughlin and Townley (1996), and Tarantola (2005).

Study objectives and the available budget will determine many of the choices made throughout the inversion process. These aspects are not incorporated in Figure 2, since it mainly serves to illustrate where interactions between geophysical and hydrological components of the inversion process might take place. In a given hydrogeophysical inversion method only a fraction of the links between the geophysical and hydrological compartments in Figure 2 is likely to be used.

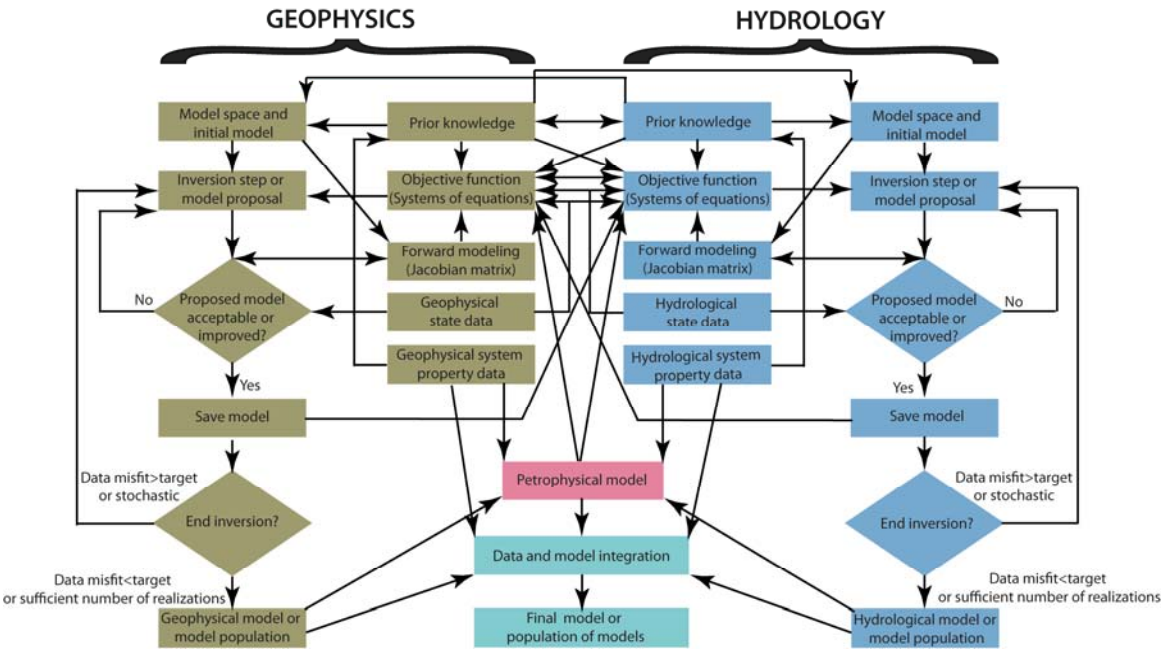

Figure 2: This flowchart illustrates possible ways that geophysics and hydrology can be integrated in hydrogeophysical studies. Recent hydrogeophysical research indicates that it is important to tightly couple hydrology and geophysics throughout the inversion and modeling process, see possible connections from blue hydrological boxes to green geophysics boxes, and vice versa. Please refer to text for details.

4.1 Key Components, Constraints, Metrics, and Steps in Parameter Estimation

Model space and initial model

A key choice in any inversion is to decide on the model parameterization used to represent the subsurface, the permissible ranges of model parameters, and the initial model (see boxes "Model space and initial model"). These choices will mainly be based upon prior knowledge (see boxes "Prior knowledge"). Prior knowledge is information about characteristics of the system that we have obtained from other sources of information than the actual geophysical or hydrogeological data that we try to invert. Prior knowledge might in this case be related to information about the

geological setting and previous exploratory or detailed studies. The link from boxes "Geophysical (or hydrological) system property data" to box "Prior knowledge" indicate also estimates of system properties that have been made outside the parameter estimation procedure (e.g., sonic log data transformed to P-wave velocities, Neutron-Neutron data transformed into porosity, EM flowmeter data translated into relative variations in permeability) and we assume that these properties are known with an associated uncertainty (Linde et al., 2006b).

Objective function (Systems of equations)

The number of independent parameters that can be inferred from hydrological and geophysical data depend on the data type, the experimental design, the number of data available, the data quality, and the forward model used. There exists however an upper limit of how many parameters one can independently estimate from a given data set. For this reason, we must find ways to constrain model space in order to obtain meaningful results, in addition to simply decrease computing time and memory use. In practice, it is necessary to explicitly constrain the parameter space by either solving an overdetermined problem with few model parameters or an underdetermined problem where a unique solution defined as the model that fits the data with the least model structure as defined by the regularization constraints used to stabilize the inverse solution. The zonation approach to model parameterization is to assume that the subsurface can be represented by a number of zones with similar physical properties, where the boundaries are either assumed to be known or are updated during the inversion process. Possible applications where a zonation approach could be justified are the delineation of sand from interbedded clay layers or sediments from the underlying bedrock. The advantage of the zonation approach is that the number of model parameters can be kept relatively small and smoothness constraints across

boundaries in the inversion may thus be avoided. The geostatistical approach is based on the assumption that the parameter field can be explained by a known or estimated spatial random variable with a certain correlation structure and deterministic trend. This parameterization is probably preferable when the parameters of interest vary in more or less random fashion and there is no clearly defined structure (see further discussion in Mclaughlin and Townley, 1996). Geophysical inversion is typically performed using a very fine model discretization where the aim of the inversion is to fit the data to a certain error level while minimizing deviations from an assumed prior model or spatial variability between neighboring cells. Regardless of the parameterization used, it is clear that prior knowledge should affect the objective function as indicated in Figure 2 (see arrow to box "Objective function (Systems of equations)").

After defining the model parameterization it is necessary to define a metric that defines what constitutes a good model and an algorithm that can be used to find such models. There are two main groups of inversion strategies: (1) deterministic inversion where one unique model is sought that describes the subsurface in some average sense (Menke, 1984; Parker, 1994); (2) stochastic inversion where a probabilistic description of the model space is used and where a large population of possible models are sampled without specifying which is the best model, only how likely they are to correspond to the available data and any prior knowledge (Tarantola, 2005). Regardless of the inversion approach, the definition of the objective function will to a large degree determine the type of models that will be obtained for a given data set.

Objective functions, at least in deterministic inversions, often include two different terms: (1) one data misfit term that characterizes how well a model explains the observed data; and (2) one

model misfit term that defines how a model corresponds with prior knowledge or any assumptions about how the model is likely to vary spatially. The most common approach is to quantify these two terms by using a least-squares formulation, where a weighted sum of the two squared misfit terms is penalized simultaneously, which typically works well when system properties are expected to vary smoothly and when data errors have an approximately Gaussian distribution. In this case, the data misfit is expressed as:

$$\chi_d^2 = \left(\mathbf{d} - \mathbf{F}[\mathbf{m}]\right)^{\mathrm{T}} \mathrm{C}_{\mathrm{d}}^{-1} \left(\mathbf{d} - \mathbf{F}[\mathbf{m}]\right), \tag{18}$$

where **d** is an $N\times1$ data vector (e.g., electrical resistances or observed drawdown at a pumping well); **F**[**m**] is a forward model operator response for a given model vector **m** of size $M\times1$; superscript T indicates transposition; $\mathrm{C}_{\mathrm{d}}^{-1}$ is the inverse of the data covariance matrix. It is commonly assumed that data errors are uncorrelated, rendering $\mathrm{C}_{\mathrm{d}}^{-1}$ a diagonal matrix that contains the inverses of the estimated variances of the data errors; thus, more reliable data carry larger weight when evaluating the data fit. The corresponding model norm is

$$\chi_m^2 = \left(\mathbf{m} - \mathbf{m}_0\right)^{\mathrm{T}} \mathrm{C}_m^{-1} \left(\mathbf{m} - \mathbf{m}_0\right), \tag{19}$$

where $\mathbf{m}_0$ is a reference model of size $M\times1$; $\mathrm{C}_{\mathrm{m}}^{-1}$ is the inverse of the model covariance matrix, which characterizes the expected variability and correlation of model parameters (Maurer et al., 1998; Linde et al., 2006a). It should be noted that it is often common to neglect the term $\mathbf{m_0}$ and replace $\mathrm{C}_{\mathrm{m}}^{-1}$ with a regularization term that approximates the square of a first or second derivative of the model. The objective function for a classical geophysical deterministic inversion is in the general least-squares case:

$$W_\lambda(\mathbf{m}) = \left(\mathbf{m} - \mathbf{m}_0\right)^{\mathrm{T}} \mathrm{C}_m^{-1} \left(\mathbf{m} - \mathbf{m}_0\right) + \lambda^{-1} \left\{\left(\mathbf{d} - \mathrm{F}[\mathbf{m}]\right)^{\mathrm{T}} \mathrm{C}_{\mathrm{d}}^{-1} \left(\mathbf{d} - \mathbf{F}[\mathbf{m}]\right)\right\} \tag{20}$$

where λ^{-1} acts as a trade-off parameter between the smooth well-conditioned problem defined by a heavy penalty on deviations from the pre-defined model behavior (i.e., λ is large) and the ill-conditioned problem defined by the data misfit term (i.e., λ is small).

In order to obtain models that display sharper contrasts over geological units or when data noise has a non-Gaussian distribution, it is possible to use a method called iteratively reweighted least-squares based on the Ekblom l_p-norm (Farquharson, 2008) thereby approaching a formulation of the inverse problem where only absolute differences in misfit are penalized, while maintaining the numerical advantages of least-squares formulations. A number of alternative data and model norms have been proposed to obtain models that provide closer representations of the expected model behavior, these methods are all based on iterative reweighting of the model misfit terms (Zhdanov, 2009; Ajo-Franklin et al., 2007; Minsley et al., 2007).

In order to evaluate the performance of a proposed model for a given objective function, it is necessary to have access to a forward model, see box “Forward modeling (Jacobian matrix)”, which is the model that numerically solves the governing partial differential equation for a given model, boundary conditions, and excitation (e.g., current injection, detonation of explosives, or water injection in a wellbore). The accuracy of the forward model is of key importance in any inversion scheme. In deterministic inversions, it is also important to have access to the Jacobian or sensistivity matrix that defines how sensitive the modeled data are to a given small perturbation of each model parameter.

The objective function offers many opportunities to couple different data types to perform joint inversion by simply augmenting **d** and **m** with new data and model types, respectively. In order to perform joint inversion, it is necessary to define some sort of constraint such that the different data types and models interact in a meaningful way. These constraints can be of many types, such as structural constraints that penalize dissimilarity between two types of models (see arrows from box “save model”). One possible approach to structural joint inversion is to assume that the gradients in two models should be parallel or anti-parallel, thereby providing models that are structurally similar (e.g., Gallardo and Meju, 2003; Gallardo and Meju, 2004; Linde et al., 2006a; Linde et al., 2008). When performing joint inversion, only one objective function is used. To decrease the number of model unknowns when solving the corresponding system of equations it is also possible to use an iterative sequential approach where two different objective functions are used as indicated in Figure 2. Another approach is to use the final model from one method to define spatial statistics that can be used to constraint the other model (Saunders et al., 2005), or the models can be constrained by using system property data from another method (Dafflon et al., 2009) or key interfaces can be incorporated, such as the depth to bedrock determined by seismic refraction in hydrogeological modeling of hill-slope processes. Such information enters the objective function through the box “Prior knowledge”.

Another approach when an accurate petrophysical relation is known to exist is to couple different model or data types by directly assuming that a given petrophysical model (known or with a given functional form with unknown parameter values) exists (see boxes “Petrophysical models”). In this way, a geophysical model can be defined by a number of hydrological properties and state variables, and the geophysical data can thereby be directly incorporated into

the hydrological inversion without the need to construct a geophysical model. In this case, only a geophysical forward model and a petrophysical model is needed to interpret the geophysical data within a hydrological inverse framework. This type of inversion methods are often referred to as fully coupled hydrogeophysical inversion (Kowalsky et al., 2005; Pollock and Cirpka, 2008). One problem with such an approach is that not only the parameter values used in petrophysical models might change within the study area, but also their functional form if they are too simplified.

Inversion step or model proposal

The next step corresponds to the boxes "inversion step or model proposal". For the deterministic case, the system of equations are solved for a given trade-off λ of the different data and model misfit terms of the objective function. A large amount of numerical methods are available to solve this problem and a review of the most common methods is outside the scope of this chapter, but a good starting point is Golub and van Loan (1996). In a typical deterministic inversion, the inversion process continue until $\chi_d^2 \approx \chi_*^2$, where χ_*^2 is a pre-defined target data misfit. A new inversion step using the model obtained in the previous model is carried out if $\chi_d^2 > \chi_*^2$, where typically also the value of λ is decreased. If $\chi_d^2 < \chi_*^2$, it is customary to repeat the previous inversion step with a larger λ until $\chi_d^2 \approx \chi_*^2$ (see boxes "End inversion?"). In cases where no convergence is obtained, one needs to change the inversion settings.

In stochastic inversions, a proposed model is evaluated based on prior knowledge and the so-called likelihood function, which is closely related to the data misfit term. Bayesian theory offers

a consistent and general framework to sequentially condition models to different data types. The posterior distribution of the model parameters **m** given data **d** is given by Bayes' theorem

$$p(\mathbf{m}\,|\,\mathbf{d}) = Cp(\mathbf{d}\,|\,\mathbf{m})p(\mathbf{m}), \tag{21}$$

where C is a normalizing coefficient, $p(\mathbf{d}\,|\,\mathbf{m})$ is the likelihood function, and $p(\mathbf{m})$ is the prior distribution of the model parameters (permissible range and the distribution within the range for each parameter). The likelihood functions provide information about how likely it is that a given model realization is responsible for the observed data.

A main attraction of Bayesian sampling methods is that virtually any formulation of the likelihood function and the prior model can be used and it can differ between data and model types if performing joint inversion. The functional form of the petrophysical relationship can also be chosen in a flexible manner. The aim of Bayesian methods is generally to explore $p(\mathbf{d}\,|\,\mathbf{m})$ and this is often done by using Monte Carlo Markov Chain (MCMC) methods (e.g., Hastings, 1970; Mosegaard and Tarantola, 1995; Chen et al., 2006; Vrugt et al., 2009).

Geophysical model or model population

Assessment of the uncertainty in the final inversion images obtained from deterministic inversion is often limited to classical linear uncertainty estimates based on the posterior model covariance matrix and resolution measures based on the resolution matrix. These estimates bear a strong imprint of the regularization used to create a stable solution (Alumbaugh and Newman, 2000). The estimated uncertainty of individual model parameters is therefore often vastly underestimated.

Different approaches have been proposed in the literature to address the variance and resolution properties of deterministic inversion models. One popular approach is simply to perform several inversions where the regularization operators or the initial model vary. This approach provides a qualitative assessment of parameters that are well resolved by the geophysical data (Oldenburg and Li, 1999). Another approach is to perform a most-squares inversion (Jackson, 1976), where the bounds within which a model parameter can vary are sought for a given small increase in data misfit. Kalscheuer and Pedersen (2007) present a non-linear variance and resolution analysis that investigate for a given variance of a model parameter, the resulting resolution properties of this estimate. The advantage compared with classical resolution analysis (e.g., Alumbaugh and Newman, 2000; Friedel, 2003) is that resolution properties are calculated for the same model variance and that regularization operators do not influence resolution estimates. Non-linearity is partly handled by introducing non-linear semi-axis that takes non-linearity in the model eigenvectors into account. Even if these methods provide a qualitative assessment of model resolution and parameter uncertainty, they provide limited insight with respect to the probability distribution of the underlying model parameters and their multi-dimensional cross-correlations.

4.2 Example Parameter Estimation Approaches

Direct mapping approaches

The simplest application of geophysical data in quantitative hydrology is direct mapping (Linde et al., 2006b). In its simplest case, all boxes and arrows related to hydrology in Figure 2 are removed and the inversion is performed using a standard geophysical inversion method. It is assumed that a known petrophysical model exists and that it can be used to map the final geophysical model into a hydrological model. Such transformations can be useful, but it is

important to understand that geophysical models are only smoothed descriptions of the real property distribution and that the estimates might be biased. Day-Lewis and Lane (2004) and Day-Lewis et al. (2005) have developed a framework to describe how resolution in geophysical images degrade as a function of experimental design and data errors for linear and linearized non-linear problems. They also show how it is possible to establish apparent petrophysical models from a known intrinsic petrophysical model that take this smoothing into account and thereby transform the geophysical model into a more realistic hydrological model. Direct mapping approaches can be made more effective when defining the model space and initial model, as well as the objective function, using prior knowledge related to the hydrology.

Integration approaches (Geostatistical, Bayesian)

A more advanced approach is to combine site-specific hydrological system property data with geophysical models. We refer to this group of models as integration approaches and they are often based on concepts from geostatistics (Linde et al., 2006b). In this case, the geophysical inversion is performed in the same way as for direct mapping, but the petrophysical model and the model integration differ. One example of this approach would be to update a model of hydraulic conductivity observed at observation wells with geophysical models that are partly sensitive to hydraulic conductivity (e.g., Chen et al., 2001). Such models can incorporate some of the uncertainty in the geophysical and petrophysical relationships in the resulting hydrological models, but they are bound to use either petrophysical models with parameters determined from laboratory measurements (which are often unsuitable in this context, Moysey et al., 2005) or empirical field-specific relationships (which may be invalid away from calibration points, Linde et al., 2006c).

Direct mapping and integration approaches are useful routine tools, but they share three main limitations: (1) laboratory-based or theoretical petrophysical models often cannot be used directly, (2) the estimation of site-specific parameter values of the petrophysical models are not included within the inversion process, (3) there is no information-sharing between different data types during the inversion, (4) resulting uncertainty estimates are qualitative at best, and (5) they often provide physically impossible models (e.g., mass is not conserved when performing tracer tests, e.g., Singha and Gorelick, 2005).

Joint inversion or fully-coupled hydrogeophysical inversion

The hydrogeophysical research community has in the last years developed approaches that do not suffer from some of the limitations of direct mapping and integration methods by using both hydrological and geophysical state data during the inversion process and by coupling the hydrological and geophysical models during the inversion. We refer to such approaches as joint inversion (Linde et al., 2006b) or alternatively, as fully-coupled hydrogeophysical inversion. These approaches often include one or more of the following: (1) hydrological flow- and transport modeling form together with geophysical forward modeling an integral part in the parameter estimation process; (2) petrophysical relationships are inferred during the inversion process; (3) non-uniqueness is explicitly recognized and a number of equally possible models are evaluated. This type of approach has at least four main advantages: (1) mass conservation can be assured in time-lapse studies and physically impossible flow fields are avoided bwhen incorporating flow- and transport simulations within the inversion framework; (2) data sharing during the inversion makes it often possible to obtain more realistic models with a higher

resolution; (3) unknown parameters of petrophysical models can be estimated during the inversion process; (4) and physically implausible model conceptualization might make it impossible to fit the data to a realistic error level. This last point is important, since it makes joint inversion well suited not only to distinguish between possible realistic models and inconsistent parameter distributions, but also between competing conceptual models. Joint inversion comes at a price since it is necessary to develop new inversion codes that are suitable to the available data and model objectives; recent hydrogeophysical joint or fully-coupled inversion methodologies include Kowalsky et al. (2005, 2006); Chen et al. (2006, 2010), Linde et al. (2006 a; 2008), Lambot et al. (2009) and Huisman et al. (2010). Such developments can in practice be greatly facilitated by incorporating freely available forward codes or by using commercial multi-physics modeling packages. Despite this, the amount of work involved is typically more significant compared with direct mapping and data integration approaches.

5. Case Studies

Several case studies are presented to illustrate the use of geophysical methods for delineating subsurface architecture (Section 5.1), delineation of anomalous subsurface fluid bodies (Section 5.2), monitoring hydrological processes (Section 5.3), and estimating hydrological properties (Section 5.4). The examples are based primarily on published hydrogeophysical studies that were conducted to gain insights about field-scale system behavior, improve flow and transport predictions, or to provide input to water resources or contaminant remediation management decisions. Examples were chosen to illustrate the utility for a variety of different characterization objectives, geophysical methods, and hydrogeophysical estimation approaches. Each example

provides a brief background of the study as well as references for readers interested in more information.

5.1 Subsurface Architecture Delineation

Because geophysical properties are often sensitive to contrasts in physical and geochemical properties, geophysical methods can be useful for mapping subsurface architecture, defined here as a distribution of hydrogeologically distinct units. Using geophysical methods for subsurface mapping is perhaps the most well-developed application in hydrogeophysics, and it is often commonly performed using surface-based geophysical techniques. Examples of common mapping objectives in hydrogeological applications include the mapping of stratigraphy or the depth to bedrock or the water table. The ability to distinguish hydrogeologically meaningful boundaries using geophysical data depends on their sensitivity to subsurface physical properties, contrasts in these properties, and the resolution of the geophysical method at the characterization target depth.

In this section, we describe the use of geophysical data for mapping subsurface architecture or features by presenting several case studies that differ in their choice of geophysical method, the scales involved, characterization objective and interpretation or integration approach. These examples include the use of airborne electromagnetic data to map lithofacies relevant for water resources at an island; high-resolution GPR imaging of braided river deposits; seismic methods to estimate subsurface architecture in contaminated environments; and fracture characterization using azimuthal SP measurements.

3D resistivity mapping of a Galapagos volcano aquifer

A fundamental limitation of most geophysical methods used in hydrogeophysics is that they have a limited ability to cover areas larger than ~1 km^2 within a reasonable time and budget at a high resolution. If funding permits, airborne geophysics can be very useful for gaining an overall view of the geological structure at the watershed scale. Most airborne data that are collected by geological surveys around the world provide only a limited depth resolution (e.g., Pedersen et al., 1994), whereas systems developed by the mining industry are designed for deeper targets and for more pronounced anomalies such that data quality demands are lower than in hydrogeological applications.

An exception is the helicopter borne SkyTEM system that was explicitly developed for mapping of geological structures in the near surface for groundwater and environmental applications (Sørensen and Auken, 2004). This is a transient electromagnetic (TEM) system that uses a strong current flowing in the transmitter coil to induce weak secondary subsurface currents whose resulting magnetic fields are subsequently measured with a receiver coil. SkyTEM measurements provide similar data quality and resolution as ground-based TEM systems, but with the advantage that measurements are carried out at speeds exceeding 15 km per hour corresponding to a typical station spacing of 35 to 45 m. This system operates normally at altitudes of 15 to 20 m with the helicopter located at an altitude of 50 m. The system is a stand-alone system that can be attached to the cargo hook of any helicopter. It uses a four-turn 12.5 × 12.5 m^2 transmitter loop with a low moment using one turn only and a high moment using all four turns. The receiver coil (0.5× 0.5 m^2) is located 1.5 m above a corner of the quadratic and rigidly fixed transmitter loop.

D'Ozouville et al. (2008) illustrate the tremendous amount of information that airborne electromagnetics can provide in hydrological studies in remote areas where only limited prior geological and geophysical work have previously been carried out. This study was motivated by the need to better understand the groundwater resources on the volcanic island of Santa Cruz in the Galapagos island, which is experiencing challenges in meeting the water demands of the island's population and its many visitors. In order to provide an overall view of potential groundwater resources at the island, a SkyTEM survey of 900 km covering 190 km^2 was carried out to obtain a detailed view of the island's internal three-dimensional electrical resistivity structure.

Figure 3 shows the resulting electrical resistivity models from two profiles that cross the island. Three-dimensional inversion of TEM data is computationally infeasible for large data sets, and the inversions were performed using one-dimensional forward modeling. The strong lateral continuity of these models is the result of lateral model constraints that are imposed during the inversion (Viezzoli et al., 2008). Four hydrogeological units were interpreted and they are indicated as I-IV in Figure 3. Unit I represents unsaturated fractured basalts with resistivities above 800 Ohm-m, Unit II is the other resistivity end-member with resistivities smaller than 10 Ohm-m representing fractured basalt invaded by sea-water. Unit III is a near-surface unit and unit IV a buried unit with resistivity values that range between 50 to 200 Ohm-m. These units might correspond to weathered zones or fractured basalts saturated with freshwater.

The top of unit II images the salt-water wedge to distances approximately 9 km inland and its slope is in perfect agreement with predictions based on the hydraulic gradient observed in one borehole and the density contrast between salt- and freshwater. Of significant hydrological interest is Unit IV that displays electrical resistivities similar to those of freshwater-saturated basalts on other islands. It forms an internal low-resistivity zone that is present only in the upper section of the southern side of the volcano. This wedge-shaped unit covers 50 km^2 and it has a thickness that varies between 10 m and 80 m. It is quasi-parallel to the topography and it coincides with the area of maximum precipitation. D'Ouzoville et al. (2008) interpret unit IV as being composed of a similar basalt as unit I, but underlain by an impermeable layer that prohibits further downward percolation.

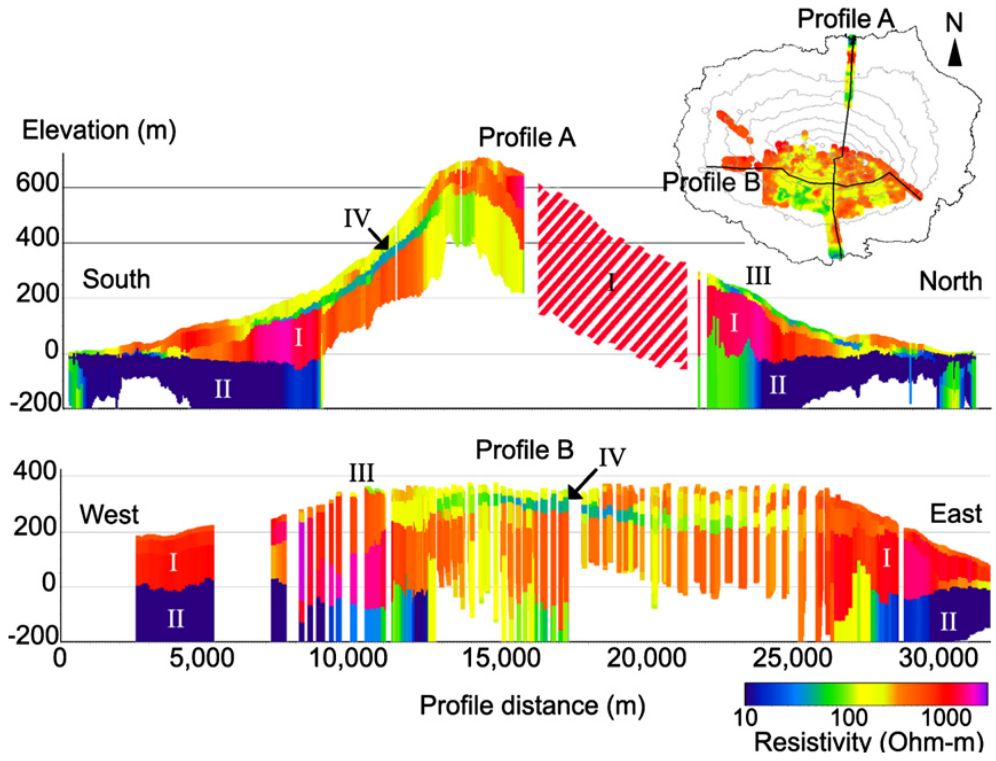

Figure 3: Two inversion models of cross-sections of Santa Cruz Island, Galapagos Islands. The positions of the south-north and west-east profiles across the island are shown on the inset over a

background of near-surface average resistivity showing extent of mapped area. The four units of hydrological interest are: (I) high-resistivity unsaturated basalts; (II) seawater intrusion wedge underlying the brackish basal aquifer; (III) near-surface, low-resistivity units consisting of colluvial deposits; (IV) internal, low-resistivity unit of saturated basalts overlying an impermeable substratum. From Figure 3 in d'Ozouville et al. (2008).

High-resolution GPR imaging of alluvial deposits.

When surface conductivity is insignificant and pore water salinity is reasonably low, one of the prime tools in near-surface (up to ten meters or so) hydrogeophysical studies is ground-penetrating radar (Davis and Annan, 1989). This method can be used to image interfaces of the three-dimensional water content distribution and can therefore be very useful to gain information about variations in water saturation in the vadose zone (Irving et al., 2009) and porosity in the saturated zone (Beres and Haeni, 1991). GPR can also be used to image fractures (Grasmueck, 1996) or investigate the depositional setting (van Overmeeren, 1998; Beres et al., 1999). The wide-spread use of GPR is mainly due to its superior vertical resolution (in the order of 0.1 to 1.0 m depending on the antenna frequency and the velocity of the subsurface) and the very fast data acquisition, which makes it possible to routinely obtain high-quality data at close to walking speed.

Gravelly, braided river deposits form many aquifers and hydrocarbon reservoirs. These deposits typically display a hierarchical architecture where permeability varies over a multitude of scales (e.g., Ritzi et al., 2004), since permeability is linked to the sediment texture, geometry, and spatial distribution of sedimentary stata. Detailed characterization of such systems is difficult,

but at least their statistical properties need to be known prior to attempting reservoir or aquifer management. In order to improve the understanding of such systems, Lunt et al. (2004) developed a three-dimensional depositional model of the gravelly braided Sagavanirktok River in northern Alaska. The data used to construct this model was obtained from cores, wireline logs, trenches and some 90 km of GPR profiles using different antenna frequencies (110 MHz, 225 MHz, 450 MHz, and 900 MHz) with corresponding depths of penetration varying from 7 m to 1.5 m. The 17 boreholes only provided limited sampling and the 1.3 km of destructive trenches provided information down to the water table only.

The GPR data provide continuous coverage over the whole thickness of the deposits and provide information about the depositional setting both across-stream and along-stream over the whole channel-belt width of 2.4 km. The GPR data made it possible to locate channel fill, unit bars, side bar deposits, confluence scour, compound braid bar deposits, and other depositional features that are of importance to understand the depositional setting. Figure 4 displays a comparison between a sedimentary log and a collocated GPR profile. Not only reflections corresponding to large scale compound bar boundaries, but also certain unit bar boundaries are clearly imaged.

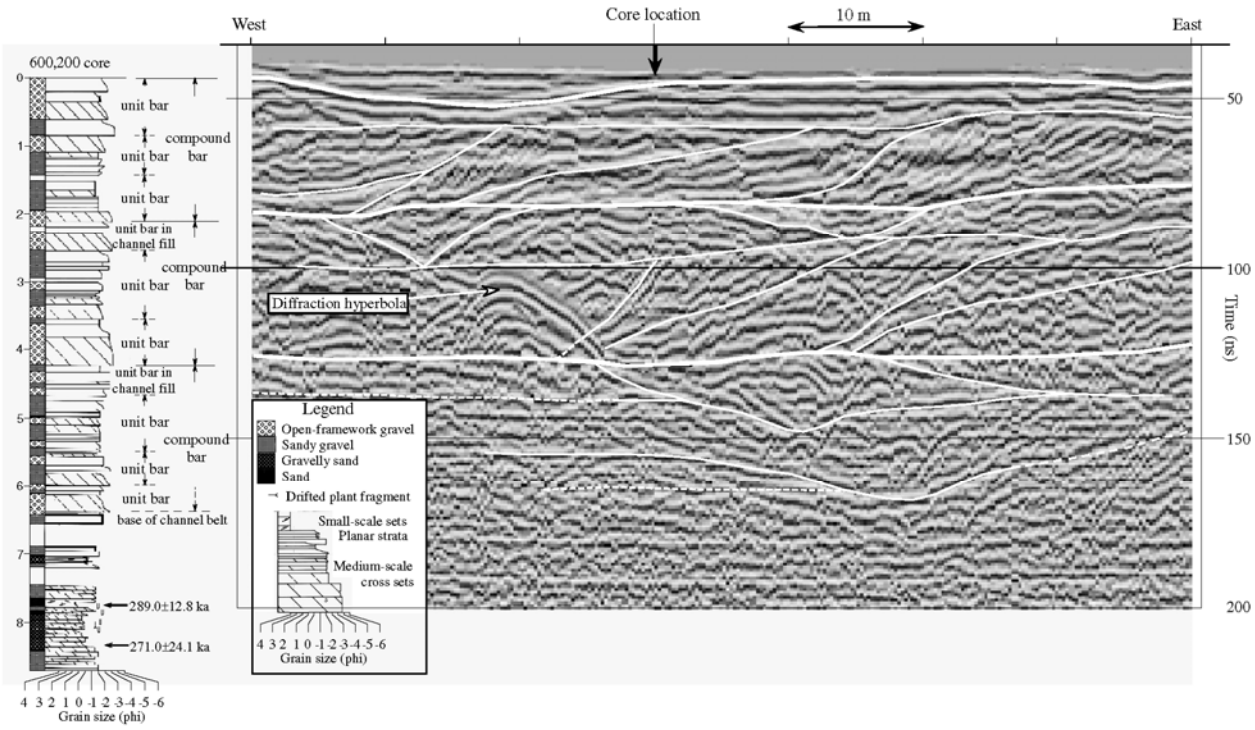

Figure 4: Comparison between a sedimentary log and a GPR profile, see arrow that indicates the core location on the GPR profile. GPR profile has a vertical exaggeration of 5:1. Sedimentary core log shows three compound bar deposits, each comprising two or three unit-bar deposits. The additional information offered by the continuous GPR profiles is evident. (Modified from Figure 12 in Lunt et al. (2004)).

Subsurface flow architecture delineation using seismic methods

The use of both GPR and seismic datasets typically entails the processing of the geophysical measurements into estimates of geophysical properties, such as reflectivity or velocity, followed by a comparison of the attributes with direct measurements often available from wellbores (e.g., lithological boundaries). Figure 4 illustrated a comparison between GPR reflectivity and wellbore lithological information. Although this two-step method often provides useful information and takes advantage of expert knowledge, the qualitative approach can limit our

ability to quantify errors associated with the interpretation and it can lead to dramatically different interpretations of subsurface heterogeneity depending on the interpreter and the processing steps employed.

To circumvent these limitations, Chen et al (2010) developed a joint inversion method that simultaneously considers surface seismic refraction traveltimes and wellbore datasets for delineating watershed architecture that may exert an influence on contaminant plume mobility at the Oak Ridge National Laboratory site in Tennessee. The groundwater at this site includes uranium, nitrate, and other contaminants that emanated from a seepage basin (S-3 ponds, Figure 5). Underlying the seepage basin is weathered and fractured saprolite that overlies bedrock. Flow is expected to preferentially occur through the more intensely weathered and fractured saprolitic zones. It is impossible to image individual fractures on a 100 m scale. However, because the fractures occur in discrete zones at this site and because the P-wave velocity in weathered and fractured zones should be lower than the surrounding more competent rock (e.g., Mair and Green, 1981, Chen et al., 2006, Juhlin and Stephens, 2006), seismic methods hold potential for aiding in the delineation of preferential flow zones.

A Bayesian joint inversion approach was developed and tested at two locations within the watershed to delineate architecture that may be important for controlling plume scale transport. Within the developed framework, the seismic first-arrival times and wellbore information about key interfaces were considered as input. A staggered-grid finite-difference method was used to forward model the full seismic waveform in 2D with subsequent automated travel-time picking. Seismic slowness and indicator variables of key interfaces are considered as unknown variables

in the framework. By conditioning to the seismic travel times and wellbore information, Chen et al. (2010) estimated the probability of encountering key interfaces (i.e., between fill, weathered saprolite low-velocity zone, and consolidated bedrock) as a function of location and depth within the watershed. An example of the results obtained from two surface seismic datasets collected along the watershed reveal the presence of a distinct low velocity zone that is coincident with the trend of the plume axis (Figure 5). This example illustrates how the joint inversion approach can explicitly incorporate wellbore data into the inversion of the seismic travel time data in the estimation of aquifer architecture at the watershed scale. Although not shown, the approach also provides estimates of uncertainty about the location of the interfaces.

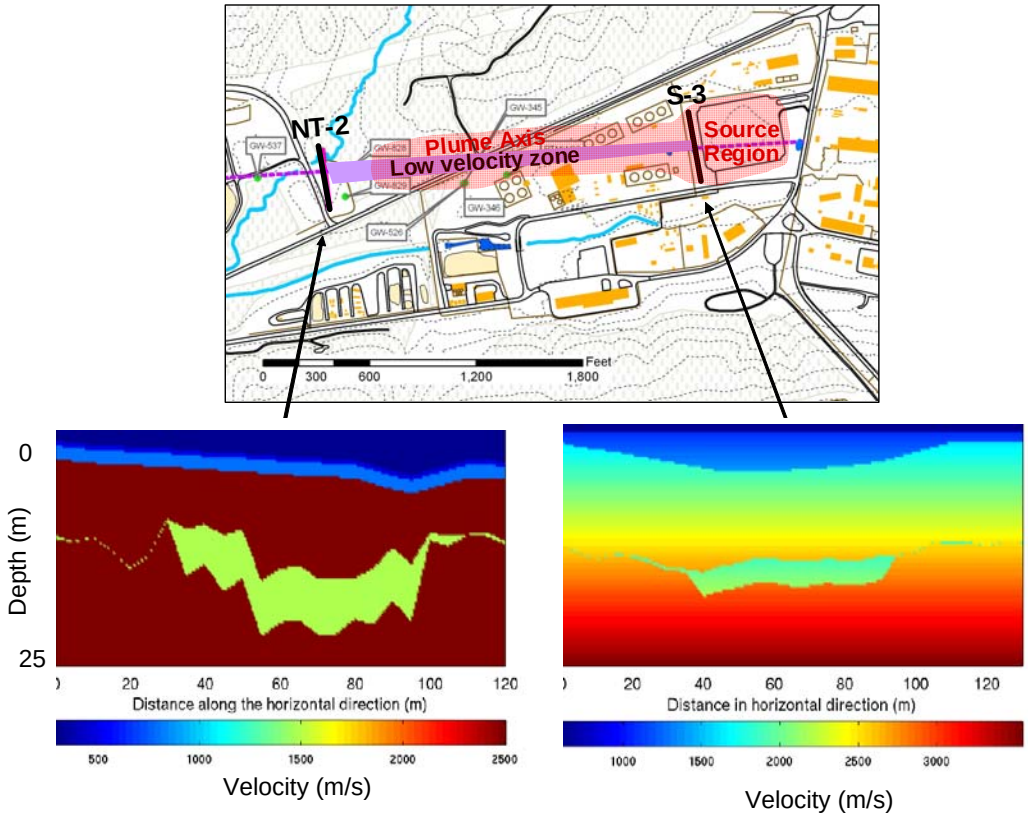

Figure 5. Bottom: Examples of seismic velocity models and subsurface architecture obtained through joint stochastic inversion of wellbore and surface based seismic refraction datasets, which reveal distinct low velocity zones that are laterally persistent along the plume axis. Top:

Superposition of low velocity zone region (shown in purple) on top of plume distribution (shown in pink), suggesting low velocity zone on plume migration. Modified from Chen et al., (submitted, 2010).

Fracture Zonation characterization using azimuthal /electrical methods

A significant body of literature has developed on using azimuthal electrical resistivity soundings to determine anisotropic electrical properties in fractured media (e.g., Taylor and Flemming, 1988; Lane et al., 1995). Electrical anisotropy in such systems is due to preferential fracture orientations, variable aperture distributions with azimuth, or clay-filled fractures. Field data suggest that directions of electrical anisotropy can under certain conditions be linked to anisotropy in hydraulic transmissivity (e.g., Taylor and Flemming, 1988), and it could therefore serve as an important data source in hydrogeological applications in fractured rock systems. Watson and Barker (1999) show that many of the electrode configurations that have been employed in past azimuthal resistivity surveys cannot discriminate between electrical anisotropy and heterogeneity. This problem can be avoided by using certain specialized electrode configurations. Unfortunately, data collection is very slow and no inversion for anisotropic parameters using such surveys has been performed to date. Linde and Pedersen (2004) demonstrate how these problems can be avoided by employing a frequency-domain electromagnetic method, namely radio magnetotellurics. Despite these methodological developments to estimate azimuthal electrical anisotropy, it is not guaranteed that electrical anisotropy coincides with preferred hydrological flow directions and any such relationship is likely to be site-specific.

Wishart et al. (2006, 2008) introduced the azimuthal self-potential gradient (ASPG) method, which provides data that may be sensitive to dominant hydrological flow directions in fractured media. In ASPG, one electrode is successively moved in steps on the order of 10° on the perimeter of an inner circle while the reference electrode moves with steps of the same size on the perimeter of an outer circle with the same midpoint as the inner circle. If the underground is predominantly anisotropic, the data will display a 180° symmetry except for data errors, while a 360° symmetry appears for measurements where lateral heterogeneity dominates. Wishart et al. (2008) applied this technique to four different fractured rock field sites in the New Jersey Highlands and found that three sites showed ASPG response that compared well with observed fracture patterns at the sites. Figure 6 shows an example from one of the sites where the self-potential data display a significant 180° symmetry indicating that large-scale fracture anisotropy is responsible for the observed ASPG data. It is also seen that the direction of the anomalies corresponds well with the mapped fracture directions at outcrops within 100 m of the measurement locations. The data from an azimuthal resistivity survey using an asymmetric arrow type array (Bolshakov et al., 1997) do not seem to correspond to either of the dominant fracture directions and the data are strongly non-symmetric, indicating that lateral variations in the electrical conductivity structure dominate. It is reasonable to assume that the positive lobes of the ASPG data indicate groundwater flow directions, but no detailed field evidence is available to confirm this even if regional flow considerations point in this direction. The magnitudes of the SP signals presented by Wishart et al. (2008) are rather large (e.g., up to 300 mV over distances of 36 m) and the variations of ASPG signals with offset are sharp. The large magnitudes can partly be explained by the shallow water table (~0.5 m) and only a few meters of till overlying the highly resistive fractured rock mass. Applications in locations with thicker and more

conductive overburden and with a deeper location of the source current will likely result in much smaller magnitude and a less clear-cut interpretation even for identical flow and fracture conditions. The usefulness of this technique in other field-settings need to be assessed, but it appears that the ASPG technique can be a very rapid method to non-intrusively map preferential flow paths in fractured rock at shallow depths where overburden thickness is thin.

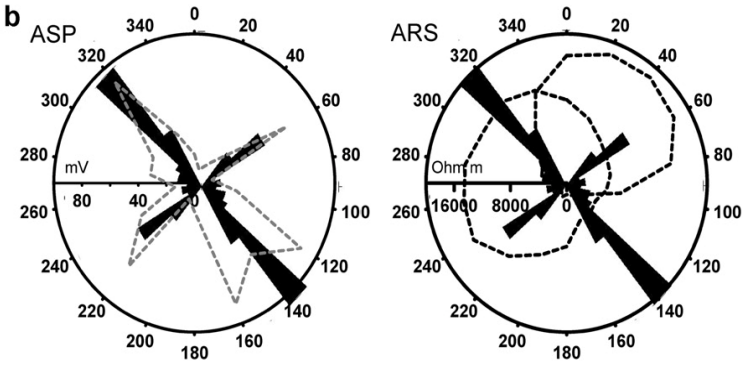

Figure 6: Azimuthal self-potential and resistivity data superimposed on rose diagrams of fracture strike sets mapped at the Wawayanda State Park, New Jersey. From Figure 4 in Wishart et al. (2008).

5.2 Delineation of Anomalous Fluid Bodies

Geophysical methods, particularly those collected from the ground-surface or from aircrafts (e.g., Paine et al., 2003), have been successfully used to identify anomalous subsurface fluid bodies, such as contaminant plume boundaries and regions impacted by salt water intrusion. Here, we illustrate the use of surface electrical approaches for delineating high ionic strength plumes and for characterizing redox gradients associated with contaminant plumes.

Electrical resistivity to delineate high ionic strength plume boundaries

Because of the strong positive correlation between total dissolved solids (TDS) and the electrical conductivity of the pore fluid, electrical methods are commonly used to delineate subsurface plumes having high ionic strength (e.g., Watson et al., 2005; Adepelumi et al, 2005; and Titov et al., 2005). As shown in Equation (5), electrical resistivity responds to porosity and surface conduction (often linked to lithology) as well as to saturation and pore fluid ionic strength. As described by Atekwana et al. (2004), activity of the natural microbial population can also impact the electrical resistivity through facilitating processes such as mineral etching, which appear to be more prevalent at the fringes of organic plumes. If the contrast between the concentration of the groundwater and the plume is great enough so that other contributions are considered to be negligible, electrical methods can be used, at least in the absence of significant clay units, to indicate contrasts in pore water electrical conductivity, or to delineate approximate boundaries of high ionic strength plumes.

An example of the use of inverted surface electrical resistivity data to delineate a deep (~50m) nitrate plume at the contaminated Department of Energy (DOE) Hanford Reservation in Washington is given by Rucker and Fink (2007). They collected six ERT transects (each at least 200 m long), inverted the data to estimate the electrical resistivity distribution in the contaminated region, and compared their results with wellbore borehole measurements of pore water electrical conductivity and contaminant concentrations. They found a strong, negative correlation between electrical resistivity and nitrate concentration above a threshold value, which was used with the electrical models to delineate the plume. Figure 7 shows several of the

inverted transects as well as the correlation between electrical resistivity and nitrate concentration obtained from co-located electrical and wellbore measurements.

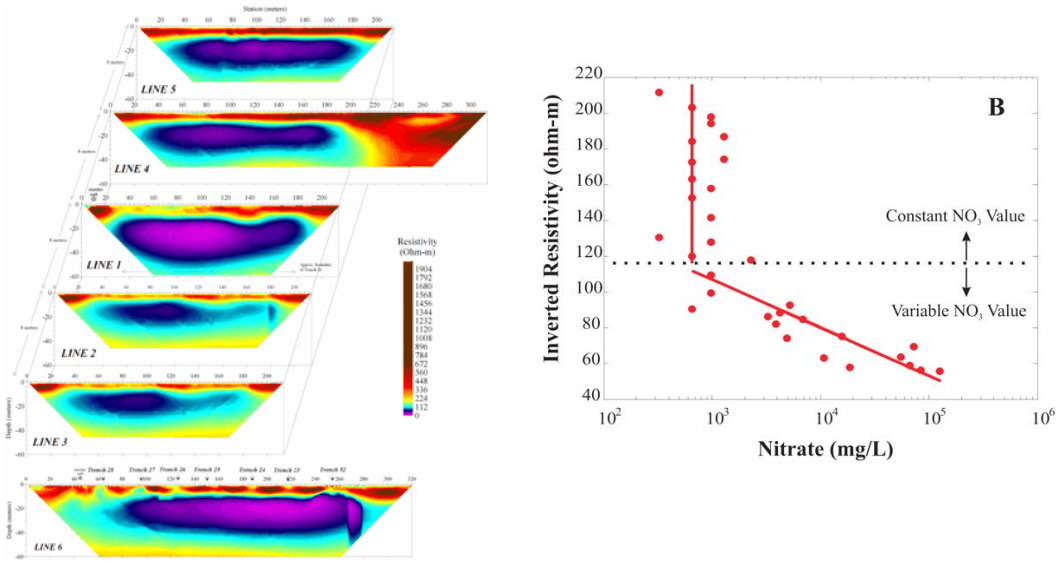

Figure 7. (a) inverted electrical resistivity profiles at the BC crib area of the contaminated Hanford, Washington Reservation, where the low electrical resistivity (high electrical conductivity) regions were interpreted as the plume; (b) observed relationship between electrical conductivity and nitrate concentration at a single wellbore location (modified from Rucker and Fink, 2007).

SP imaging of redox potentials associated with contaminated plumes

The traditional application of the self-potential method has been in mineral exploration where large negative self-potential anomalies are typically associated with mineral veins (Fox, 1830). As an extreme example, Goldie (2002) presents a peak anomaly of -10.2 V associated with highly resistive high-sulfidation oxide gold deposits. The main contribution of such anomalies is

thought to be related to electrochemical half-reactions (Sato and Mooney, 1960; Bigalke, 1997), even if it has been suggested that some field data contradict this model (Corry et al., 1985).

Naudet et al. (2003, 2004) observed large negative self-potential anomalies over the Entressen domestic landfill outside Marseille, France. Redox potential, or Eh, indicates the tendency for oxidation-reduction reactions to occur. Strong redox gradients often become established adjacent to contaminant plumes. They found that the residual self-potential data (Figure 8a), where the effects of streaming currents had been filtered out, were strongly correlated with the difference in redox potential between groundwater samples in the contaminated landfill and uncontaminated areas. They invoked an explanation in analogy with the models of Sato and Mooney (1960) and Bigalke (1997).

To remotely map variations in redox potential, Linde and Revil (2007) developed a linear inversion model where the difference in redox potential is retrieved from the residual self-potential data assuming a known one-dimensional electrical resistivity model and a known depth at which electrochemical reactions take place. They created a simplified representation of the electrical conductivity structure of the Entressen landfill based on ERT models and they assumed that source currents are located at the water table. Figure 8b shows a comparison between the simulated and observed residual self-potential data of Naudet et al. (2003, 2004). Figure 8c displays the retrieved redox potentials assuming a known background value outside of the contaminated area. By comparing these estimates and measured redox potentials in the wells (Figure 8d), they found that the inversion results can retrieve the measured redox potentials quite well given the simplifying assumptions involved. It should be noted that equally good data fits

between the simulated and observed self-potential data could have been achieved by shifting the depth at which the sources are imposed or by assuming that the vertical dipole sources are distributed over a volume and not over an area (Blakely, 1996). The interpretation of self-potential data must therefore be treated with caution and significant prior constraints must be imposed. Nevertheless, it appears that SP mapping and monitoring may provide a cheap and reliable method for monitoring field scale distribution of redox potential at contaminated sites. It is necessary that this approach is tested at other research sites before its applicability can be properly assessed.

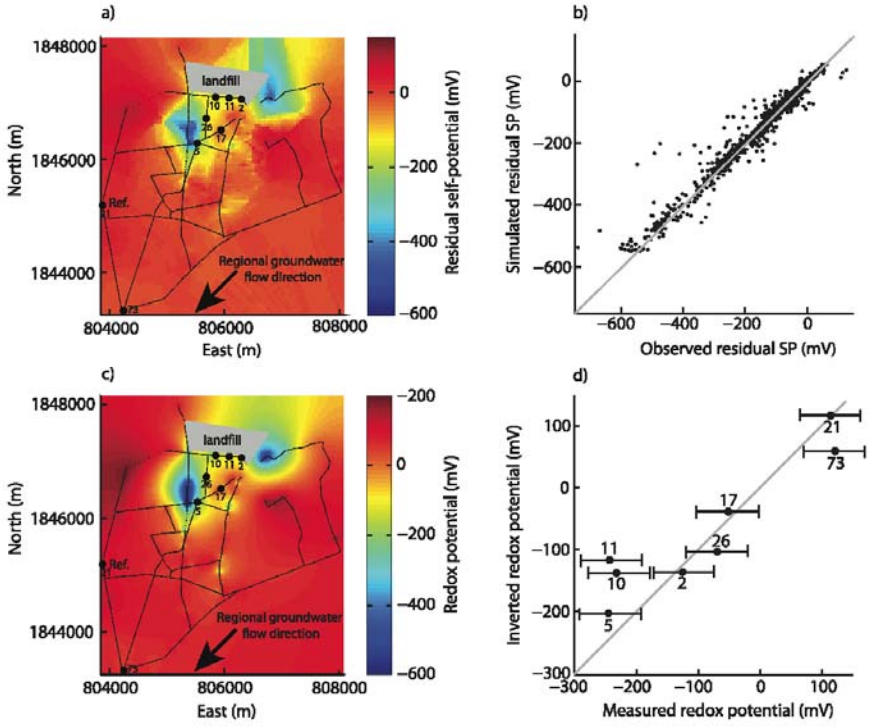

Figure 8: (a) Residual SP map at the Entressen landfill, in which the black lines indicate the SP profiles (2417 SP measurements). (b) Comparison of simulated SP with the residual SP estimated from the measured SP data. The response of the inverted model fits the residual SP to the estimated standard deviation. (c) Inverted redox potential in the aquifer at Entressen. (d)

Comparison of inverted redox potentials in the aquifer with in situ measurements from Entressen (the correlation coefficient is 0.94). Modified from Linde and Revil (2007) by permission of the American Geophysical Union.

5.3 Hydrological Process Monitoring

A particularly powerful component in hydrogeophysics is the use of a suite of geophysical datasets, collected at the same locations as a function of time, to monitor hydrological processes. Such repeated studies are often referred to as 'time-lapse' geophysics, and their advantages compared to static images are significant for process monitoring. First of all, changes in well-designed time-lapse inversions are most often primarily related to changes in state variables only (e.g., temperature, pressure, partial saturations of different phases, and the electrical conductivity of the pore fluid) and not to characteristics of the rock matrix itself. Time-lapse imaging has also the advantage that errors in the forward model tend to cancel (e.g., LaBrecque and Yang, 2001; Lien and Mannseth, 2008). It should be noted that subsurface engineered manipulations, such as those associated with environmental remediation, aquifer storage and recovery, and carbon sequestration can indeed alter the physical properties of the material. For example, remediation treatments can induce biogeochemical transformations that in turn alter the pore geometry and ultimately the fluid flow characteristics (Englert et al., 2009; Li et al., 2009). The geophysical responses to such processes are currently under intense study in the research area of biogeophysics (Atekwana et al., 2006; Williams et al., 2005; Chen et al., 2009, Slater et al., 2009), but are not covered in this chapter.

Below, we present several examples that illustrate the use of time-lapse geophysics, including: GPR to monitor the spatiotemporal distribution of soil water content in agricultural and hillslope settings; the use of GPR to monitor the distribution of saline tracers in fractured rock; and the use of electromagnetic methods to monitor seasonal changes in freshwater-seawater dynamics.

Soil moisture monitoring

The vadose zone mediates many of the processes in the hydrological cycle, such as: the partitioning of precipitation into infiltration and runoff, groundwater recharge, contaminant transport, plant growth, evaporation, and sensible and latent energy exchanges between the Earth's surface and its atmosphere. As an example, in catchment hydrology, the readiness of an area to generate surface runoff during storm rainfall is related to its surface storage capacity. Given the predominant effects of soil moisture on the production of crops, soil salinization, carbon cycling, and climate feedback, development of methods for monitoring moisture content over field-relevant scales is desirable (e.g., Vereecken et al., 2008). Equations (4) and (12) indicate that both the dielectric constant and electrical conductivity are sensitive to water content. Because of this sensitivity, geophysical methods that are sensitive to these properties (e.g., GPR and ERT) have been used fairly extensively to monitor the spatiotemporal distribution of soil moisture.

As described by the reviews given by Huisman et al. (2003) and Lambot et al. (2008), GPR is commonly used in hydrogeophysical studies to estimate water content. Various GPR waveform components and configurations have been used to estimate water content, including: crosshole radar velocity (Hubbard et al., 1997; Binley et al., 2002b), surface ground wave velocity (Grote

et al., 2003), subsurface reflection (Greaves et al., 1996; Lint et al., 2005), and air-launched ground-surface reflection approaches (Lambot et al., 2006). An example of the use of time-lapse surface reflection GPR coupled with a Bayesian method to estimate seasonal changes in water content in the root zone of an agricultural site is given by Hubbard et al. (2006). Within a 90m × 220m section of this agricultural site, a thin (~0.1 m), low permeability clay layer was identified from borehole samples and logs at a depth of 0.8 to 1.3 m below ground surface. GPR data were collected several times during the growing season using 100 MHz surface antennas; these data revealed that the thin clay layer was associated with a subsurface channel. Following equations (1) and (15), as the bulk water content in the unit above the GPR reflector increased, the dielectric constant increased, which lowered the velocity and lengthened the two way travel time to the reflector. As a result, the GPR reflections revealed seasonal changes in the travel time to the clay layer as a function of average root zone moisture content. At the wellbore locations, a site-specific relationship between the dielectric constant and volumetric water content was used with the radar travel times to the clay reflector to estimate the depth-averaged volumetric water content of the soils above the reflector. Compared to average water content measurements from calibrated neutron probe logs collected over the same depth interval, the estimates obtained from GPR reflections at the borehole locations had an average error of 1.8% (Lunt et al., 2005). To assess seasonal variations in the root zone water content between the wellbores, the travel time picks associated with all GPR datasets, the wellbore information about the depths to the clay layer, and the site-specific petrophysical relationship were used within a Bayesian procedure (Hubbard et al., 2006). Figure 9 illustrates the estimated volumetric water content for the zone located above the reflecting clay layer at different times during the year. The figure indicates seasonal variations in mean water content and also that the channel-shaped feature influences

water content distribution: within this area the soils are consistently wetter than the surrounding soils. The soil moisture variations appeared to play a significant role in the crop performance: crops located within the channel region had consistently higher crop weight relative to the surrounding regions. These results suggest that the two-way GPR reflection travel times can be used to obtain estimates of average soil layer water content when GPR reflectors are present and when sufficient borehole control is available.

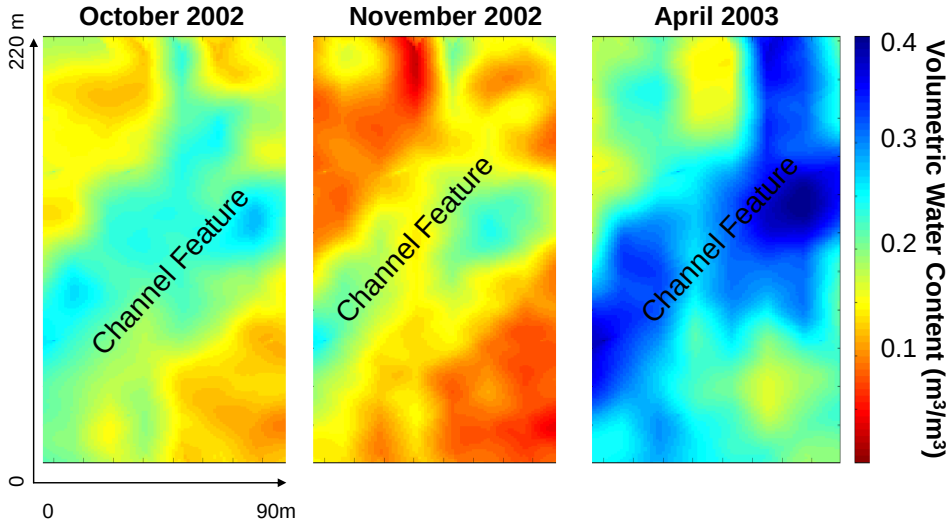

Figure 9 Plan view map of average volumetric water content of the top soil layer (<1.5m below ground surface) at the agricultural study site, estimated using 100 MHz GPR reflection travel time data and borehole neutron probe data within a Bayesian estimation approach. Color key at right indicates relative volumetric water content, from red (drier) to blue (wetter). Modified from Hubbard et al. (2006).

Several studies have also explored the use of surface ERT datasets for characterizing moisture infiltration and redistribution at the hillslope and watershed scales. For example, Berthold et al.

(2004) compared electrical conductivity estimates from surface ERT images with groundwater electrical conductivity measurements to evaluate the roles of wetlands and ponds on depression-focused groundwater recharge within a Canadian wildlife region. The surface electrical data revealed a complex pattern of salt distribution that would have been difficult to understand given point measurements alone. Koch et al. (2009) collected surface electrical profiles over time along 18 transects within a German hillslope environment, and used the images together with conventional measurements to interpret flow pathways and source areas of runoff.

Saline tracer monitoring in fractured rock using time-lapse GPR methods

Hydrogeophysical applications in fractured media are challenging because of the large and discrete variations between the physical properties of the intact rock mass and the fractures (NRC, 1996). Time-lapse imaging of geophysically detectable tracers has been used in recent years to improve the understanding of fracture distribution and connectivity. The best adapted geophysical technique to image individual fractures away from boreholes, up to some ten meters away from the boreholes, is probably single-hole radar reflection measurements. This method has been shown to be a useful tool in site characterization efforts to determine possible orientations and lengths of fractures in nuclear waste repository laboratories (Olsson et al., 1992) and in characterizing unstable rock masses (Spillmann et al., 2007). By stimulating individual fractures by adding a saline tracer, it is possible to image tracer movement from the surface (Tsoflias et al., 2001; Talley et al., 2005; Tsoflias and Becker, 2008) and in-between boreholes (Day-Lewis et al., 2003; 2006) by investigating how the amplitude of GPR signals vary over time for a given transmitter-receiver geometry while the saline tracer migrates in the rock fractures. One problem with such studies is that the data acquisition time is often comparable to

the time-scale of the hydrological flow processes in the fractures where fluid flow velocities might be very high, creating large inversion artifacts if the data acquisition time is ignored in the inversion process.

Day-Lewis et al. (2002; 2003) present an innovative inversion method for difference-attenuation crosshole GPR data where the data acquisition time is included within the inversion. Synthetic (Day-Lewis et al., 2002) and field-based (Day-Lewis et al., 2003; 2006) inversion results show significant improvements compared with classical time-lapse inversion algorithms. The research of Day-Lewis et al. (2003, 2006) was carried out at the Forest Service East (FSE) well field at the U.S. Geological Survey (USGS) Fractured Rock Hydrology Research Site located near Mirror Lake, New Hampshire. This well field consists of 14 boreholes distributed over an area of 120×80 m^2. Saline injection tests were carried out at 45 m depth where four boreholes, with side-lengths of approximately 10 m located in a square-like shape seen from above, are hydraulically connected (Hsieh and Shapiro, 1996). These tracer tests were performed using weak-doublet tracer tests, where fluid was pumped out of one borehole at a rate of 3.8 L/min and water was injected in another borehole at 1.9 L/min. After achieving steady state flow, the injection fluid was changed from freshwater to a sodium-chloride (NaCl) concentration of 50 g/L NaCl. Injection of freshwater was resumed after 10 minutes. The electrical conductivity ratio of these two fluids was estimated to be close to 170. A conventional packer system was used in the pumping well, whereas a special PVC packer system that allowed measurements while preventing vertical flow and the saline solution from entering the boreholes was used in the injection well and in two neighboring wells where GPR measurements were also conducted.

The energy of a GPR signal that arrives at the receiving antenna depends to a large degree on the electrical conductance of the media in-between the transmitting and receiving antenna. It is expected that the magnitude of the signal at the receiving antenna decreases significantly when a saline tracer passes the ray-path. Difference-attenuation inversion is a linear problem since electrical conductivity has no significant effect on the actual ray path. Figure 10 displays variations in the ray-energy that arrives in the receiver antennas normalized by the ray-length for different transmitter and receiver separations during the tracer experiment of Day-Lewis et al. (2003) for a borehole plane roughly perpendicular to the injection and pumping borehole. Figure 12 also shows the corresponding chloride concentration in the pumping well. The geophysical difference-attenuation data and the chloride data seem to agree qualitatively and a quicker "breakthrough" in the GPR data is observed because they were acquired over an area halfway between the injection and pumping boreholes.

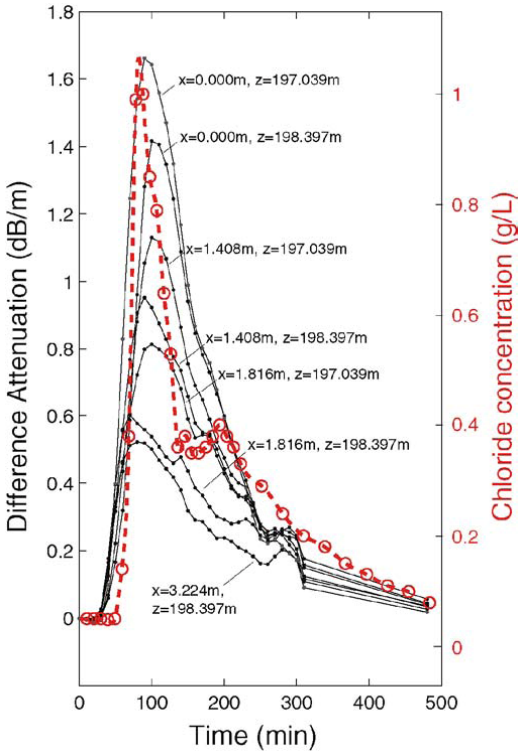

Figure 10: Nodal difference-attenuation histories between two boreholes (in black) and measured chloride concentration (in red). From Day-Lewis et al. (2006).

This type of data was later inverted by Day-Lewis et al. (2003) and they showed that it was possible to remotely monitor the tracer movement relatively well given that only three two-dimensional slices through the 3D volume could be imaged. It appears that difference-attenuation data might provide the resolution needed to study fluid flow in fractured rock with only limited hydrological point sampling.

Seasonal changes in regional saltwater dynamics using time-lapse electromagnetic methods

Falgàs et al. (2009) present one of few published time-lapse hydrogeophysical studies at the km scale (see Ogilvy et al. (2009) and Nguyen et al. (2009) for seawater intrusion studies using ERT). They used a frequency-domain electromagnetic method, namely Controlled-Source Audiomagnetotellurics (CSAMT) (Zonge and Hughes, 1991), to monitor freshwater-seawater interface dynamics in the deltaic zone of the Tordera River in northeastern Spain. Monitoring of saltwater intrusion in coastal aquifers is important due to population growth and since most of the World's population is concentrated along coastal areas. The CSAMT data were collected over an ancient paleochannel that controls seawater intrusion in a part of the delta. During two years, a profile of seven soundings was acquired along a 1700 m N-S trending line. Due to agricultural activity, they couldn't recover previous site locations with accuracy higher than 100 m when performing the repeated measurements.

The resulting individually inverted resistivity models are shown in Figure 11 together with a weighted root-mean-square (RMS) data misfit calculated with an assumed error level of 5%. To better distinguish temporal changes, the inversions used the inversion results of the first survey as initial model for the subsequent inversions. The changes of the electrical resistivity models over time clearly indicate saltwater encroachment in the low-resistivity layer at approximately 50 m depth. These dynamic processes are best imaged in the northern part of the profile where the seawater wedge retreated towards the sea from April 2004 until December 2004, followed by progression until August 2005, and finally followed by a new retreat until May 2006. Multilevel sampling of a piezometer (W06) in April 2004 displayed a saltwater content of approximately 8% at 50 m depth. Additional evidence to support the interpretation of the geoelectrical models in terms of seawater intrusion is offered by the piezometric levels that were the lowest in August 2005 when the sea-water intrusion was interpreted to be at its maximum. Another zone displaying seawater intrusion dynamics is shown in a shallow aquifer located in the upper tenths of meters close to the sea located to the South.

Even if the study of Falgàs et al (2009) had certain limitations, namely rather few stations, long-periods between measurements, and not identical measurement locations between surveys, it still shows the potential of electromagnetic methods to monitor sea-water intrusion processes on a scale that is relevant for water resources planning. Electromagnetic methods have a higher sensitivity to conductors (e.g., the sea-water plume) than the more commonly used ERT method, even if they have a poor resolving power in defining the lower boundary of conductors. This limitation can partly be resolved by combining this type of geophysical data with other types of geophysical data, such as seismic refraction data during the inversion (Gallardo and Meju, 2007).

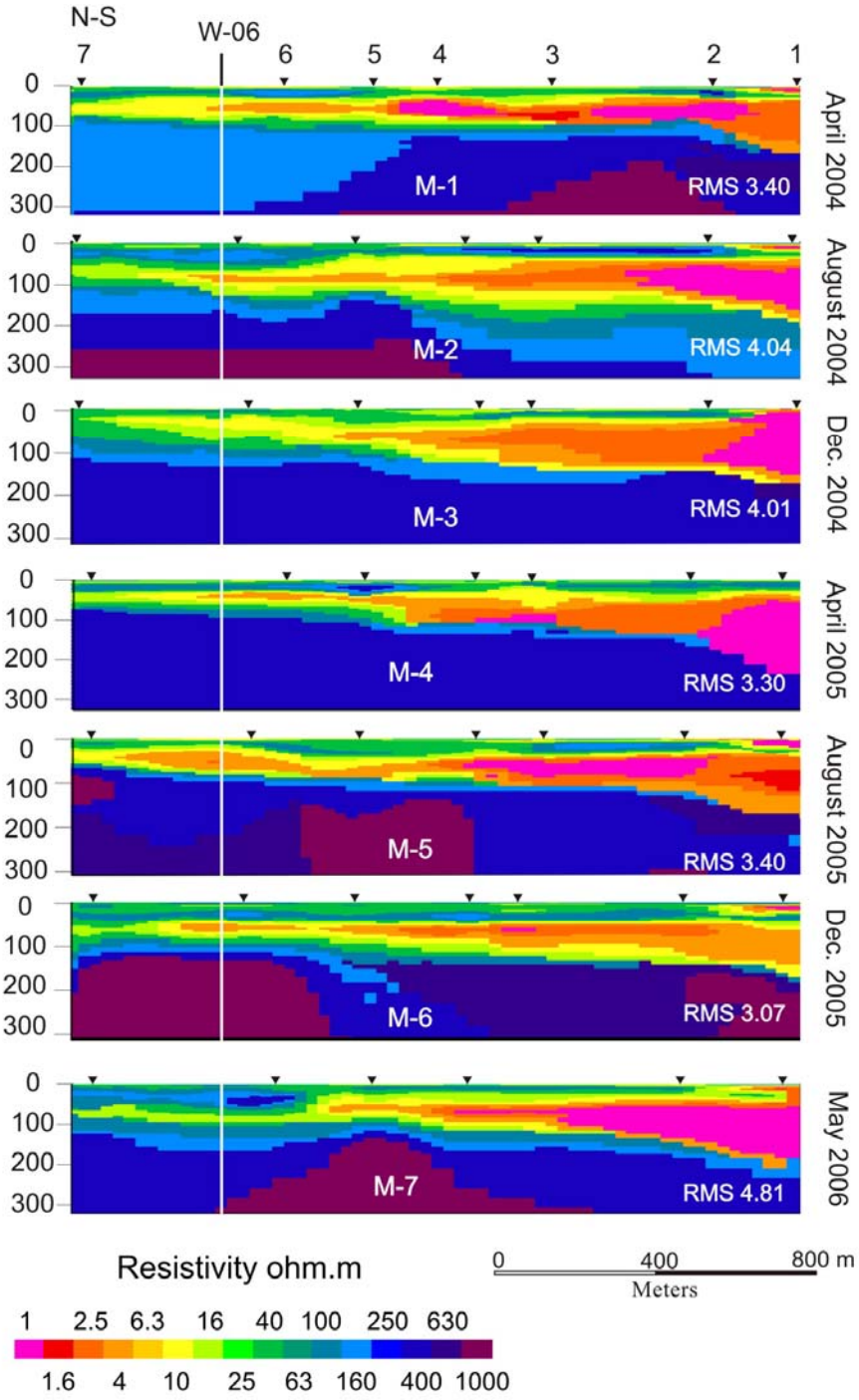

Figure 11: A series of two-dimensional electrical conductivity models as a function of date, with the triangles indicating survey location and the y-axis depth in m. From Falgàs et al. (2009).

5.4 Hydrogeological Parameter or Zonation Estimation for Improving Flow Predictions

Developing a predictive understanding of subsurface flow is complicated by the inaccessibility of the subsurface, the disparity of scales across which controlling processes dominate (e.g., Gelhar, 1993) and the sampling bias associated with different types of measurements (e.g., Scheibe and Chien, 2003). In this section, we describe the use of geophysical methods to improve flow predictions, though improved parameterization of flow and transport models as well as through fully-coupled hydrogeophysical inversion. Although the examples provided here have been conducted at the local scale, joint or fully-coupled hydrogeophysical inversion at the watershed scale is a research area that we expect to become more advanced coming years.

Hydraulic conductivity and zonation estimation using GPR and seismic methods

Several studies have described the use of geophysical data for estimation of hydraulic conductivity (e.g., Cassiani et al., 1998; Hyndman et al., 2000; Hubbard et al., 2001; Chen et al., 2001; Gloaguen et al., 2001; Slater, 2007; Linde et al., 2008). A few studies have also illustrated the value of geophysically-obtained information for improving flow and transport predictions (Scheibe and Chien, 2003; Bowling et al., 2006; Scheibe et al., 2006). One such example is provided by the linked hydrogeophysical-groundwater modeling study performed at the DOE Oyster Site in Virginia. At this site, tomographic data were used together with borehole flowmeter logs to develop a site-specific petrophysical relationship that linked radar and seismic velocity with hydraulic conductivity. Using a Bayesian approach, a prior probability of hydraulic conductivity was first obtained through geostatistical interpolation (i.e., kriging) of the hydraulic conductivity values obtained at the wellbore location using the flowmeter logs. Within the Bayesian framework, these estimates were then ‘updated’ using the developed petrophysical

relationship and estimates of radar and seismic velocity obtained along the tomographic transects (Figure 12). The method yielded 'posterior' estimates of hydraulic conductivity (and their uncertainties) along the geophysical transects that honored the wellbore measurements (Chen et al., 2001; Hubbard et al., 2001). Examples of mean values of the geophysically-obtained hydraulic conductivity estimates are shown in Figure 12, where the transects are oriented parallel and perpendicular to geological strike. The estimates were obtained at the spatial resolution of the geophysical model, which had pixel dimensions of 0.25 m × 0.25 m.

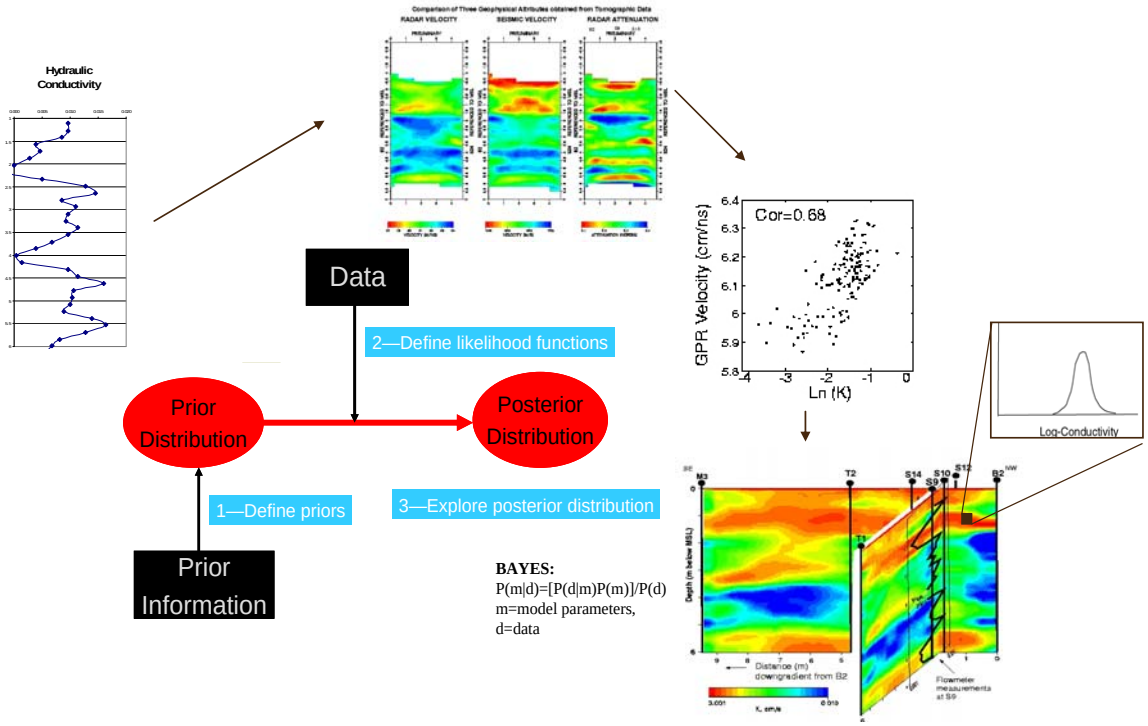

Figure 12. Example of Bayesian approach for integrating disparate datasets for the estimation of hydraulic conductivity distributions, where the mean value of the estimated hydraulic conductivity distributions is shown on the bottom right (Modified from Hubbard et al., 2001).

The geophysically-obtained estimates were then used to develop a synthetic aquifer model (Scheibe and Chien, 2003). Other types of datasets were also used to develop other aquifer models, including interpolated core hydraulic conductivity measurements and interpolated flowmeter data. The breakthrough of a bromide tracer through these different aquifer models was simulated and subsequently compared with the breakthrough of the bromide tracer measured at the Oyster site itself (Scheibe and Chien, 2003). Even though this site was fairly homogeneous (the hydraulic conductivity varied over one order of magnitude) and had extensive borehole control (i.e., wellbores every few meters), it was difficult to capture the variability of hydraulic conductivity using borehole data alone with sufficient accuracy to ensure reliable transport predictions. Scheibe and Chien (2003) found that "conditioning to geophysical interpretations with larger spatial support significantly improved the accuracy and precision of model predictions" relative to wellbore based datasets. This study suggested that the geophysically based methods provided information at a reasonable scale and resolution for understanding field-scale processes. This is an important point, because it is often difficult to take information gained at the laboratory scale or even from discrete wellbore samples and apply it at the field scale.

The level of detail shown in the hydraulic conductivity estimates of Figure 12 may not always be necessary to adequately describe the controls on transport; in some cases, defining only contrasts between hydraulic units (Hill, 2006) or the hydraulic zonation may be sufficient to improve flow predictions. Several studies have illustrated the utility of tomographic methods for mapping zonation of lithofacies or hydrologically-important parameters. Hyndman et al. (1996) jointly used tracer and seismic tomographic data to map hydrological zonation within an alluvial aquifer. Linde et al. (2006c) used tomographic zonation constraints in the inversion of tracer test

data and found that the constraints improved hydrogeological site characterization. Hubbard et al. (2008) used a discriminant analysis approach to estimate hydraulic conductivity zonation at the contaminated Hanford 100H site, and found that the identified heterogeneity controlled the distribution of remedial amendments injected into the subsurface for bioremediation purposes as well as the subsequent biogeochemical transformations.

Joint modeling to estimate temporal changes in moisture content using GPR

In this example, we illustrate the value of the joint inversion approach for taking advantage of the complementary nature of geophysical and hydrological data and to circumvent some of the obstacles commonly encountered in other types of integration approaches (see section 4.2). As was previously discussed, the use of GPR methods for mapping water content distributions in the subsurface is now well established. However, in general, GPR measurements cannot be directly related to the soil hydraulic parameters needed to make hydrological predictions in the vadose zone (such as the permeability and the parameters describing the relative permeability and capillary pressure functions). On the other hand, time-lapse GPR data often contain information that can be indirectly related to the soil hydraulic properties, since these soil hydraulic properties influence the time- and space-varying changes in water distribution, which in turn affect GPR data.

Kowalsky et al. (2004, 2005) illustrated an approach for incorporating time-lapse GPR and hydrological measurements into a hydrological-geophysical joint inversion framework for estimating soil hydraulic parameter distributions. Coupling between the hydrological and GPR simulators was accomplished within the framework of an inverse model (iTOUGH2, Finsterle,

1999). The inversion was performed using a maximum *a posteriori* (MAP) approach that utilized concepts from the pilot point method. One of the benefits of this approach was that it directly used the GPR travel times rather than radar velocity tomograms, which circumvented some of the problems that were discussed in Section 4.2. The approach also accounted for uncertainty in the petrophysical function that related water content and dielectric permittivity.

The approach was applied to data collected at the 200 East Area of the U.S. Department of Energy (DOE) Hanford site in Washington. The Hanford subsurface is contaminated with significant quantities of metals, radionuclide, and organics; contaminants are located in the saturated as well as in a thick vadose zone. Gaining an understanding of vadose zone hydraulic parameters, such as permeability, is critical for estimating plume infiltration at the site and the ultimate interception with groundwater and the nearby Columbia River. To gain information about the vadose zone hydraulic parameters, an infiltration test was performed by ponding water on the ground surface and subsequently measuring the subsurface moisture distribution over time using neutron probe data collected within wellbores and radar tomographic data collected between boreholes (Figures 13a and b).

Because water infiltration behavior is a function of the permeability distribution, the joint inversion procedure could be used with the time-lapse moisture data to estimate log-permeability. The inversion procedure was also used to estimate other parameters of the petrophysical relationship, porosity, and the injection rate, none of which were measured precisely at the site. Figure 13c illustrates the permeability values estimated from the joint inversion procedure, which have been conditioned to GPR travel times and to the measured

hydrological properties. The obtained permeability values were then used to predict fluid flow at future times. The accuracy of predictions for future times was evaluated through comparison with data collected at later times but not used in the inversion. In the first case, inversion was performed using only neutron probe data collected in two wells at three different times. In the second case, inversion was performed using GPR data collected at two times in addition to the neutron probe data used in the first case. Compared to predictions made through inversion of only neutron probe data, inclusion of GPR data in the joint inversion resulted in more accurate estimates of water content at later times.

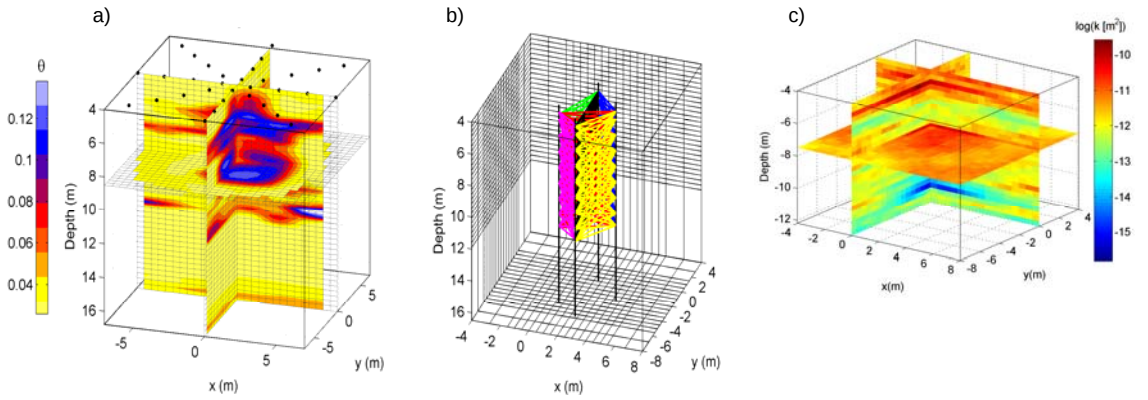

Figure 13. Time-lapse data sets collected during water injection at Hanford site including (a) interpolated water content inferred from dense neutron-probe measurements and (b) ground-penetrating radar acquisition geometry. Estimates of log-permeability (c) obtained using the coupled inversion approach (modified from Kowalsky et al., 2006).

6. Summary and Outlook

This chapter has reviewed several case-studies that illustrated how hydrogeophysical methods can be used to: map subsurface architecture, estimate subsurface hydrological properties or state variables, and monitor subsurface processes associated with natural or engineered *in-situ* perturbations to the subsurface system. These and many other studies have now demonstrated that hydrogeophysical approaches can successfully be used to gain insight about subsurface hydrological processes, provide input that improves flow and transport predictions, and provide information over spatial scales that are relevant to the management of water resources and contaminant remediation. Critical to the success of hydrogeophysical studies are several factors: (1) the acquisition of high-quality geophysical data; (2) the availability of petrophysical relationships that can link geophysical properties to the parameters or processes relevant for the hydrological study; and (3) the use of inversion approaches that allow for reliable and robus estimation of hydrological parameters of interest. Here, we briefly comment on each of these important factors and associated research needs.

Section 2 reviewed many of the geophysical methods that are common or are being increasingly employed in hydrogeophysical studies, including: electrical resistivity, induced polarization, controlled source inductive electromagnetic, self potential, ground penetrating radar, seismic, surface nuclear magnetic resonance, gravity, magnetics, and well logging methods. We stressed that acquisition of high-quality data is critical to a successful hydrogeophysical study. The choice of which geophysical data to invoke for a particular investigation must be made based on the expected sensitivity of the geophysical attribute to the properties associated with the characterization objective (or the contrast of the target properties with the surrounding sediments

or rocks). Different geophysical methods perform optimally in different environments and have different resolving capabilities. It is thus necessary, when deciding on which geophysical method to use to consider the general geological setting and the size/depth/contrast magnitude of the characterization target. Although these characteristics should be considered prior to choosing a method (and ideally considered through synthetic modeling), commonly the performance of a geophysical method can not be truly assessed until it is tested at a particular field site. This is because factors that influence its performance (such as clay content, depth of particular target, contrast in characterization target properties with surrounding material, and presence of cultural features such as underground pipes) are often not known with sufficient certainty prior to field testing. For this reason, geophysical campaigns are ideally performed in an iterative manner, starting first with reconnaissance campaigns that involve testing the geophysical responses of a few different methods prior to choosing the method for further high-resolution investigation.

Section 3 described common petrophysical models that link electrical conductivity, dielectric permittivity, complex conductivity, and self potential measurements to hydrological variables, which are commonly based on theoretical considerations or on laboratory- or field-based experiments. Unfortunately, all of these petrophysical model types pose challenges for hydrogeophysical studies. Theoretical models often invoke assumptions or simplifications that deviate from heterogeneous, *in-situ* conditions. Problems with laboratory-based measurements (e.g., Ferré et al., 2005) are that it is very difficult to (1) acquire undisturbed samples that adequately represent conditions in the near subsurface and to (2) upscale developed relationships from the laboratory to the field scale (Moysey et al., 2005). Application of field-scale relationships (e.g., using co-located hydro-geophysical wellbore datasets; Hubbard et al., 2001)

can also be problematic if the petrophysical relationship differs at locations away from the wellbore (Linde et al., 2006c). Finally, because most geophysical attributes are sensitive to more than one property that typically varies substantially in the subsurface, methods must be developed to handle non-uniqueness in geophysical responses to property variations (Hubbard and Rubin, 1997). The development and testing of petrophysical relationships that describe the linkages between field-scale geophysical responses to variably saturated, semi- to un-consolidated, low pressure materials that typify many of our shallow subsurface environments continues to be a need in hydrogeophysics. Embedded in that need is the development of methods that can adequately handle scale-effects, non-uniqueness, and uncertainties associated with petrophysical relationships.

The importance of parameter estimation/integration methods that honor available hydrogeological and geophysical data in the interpretation procedure was described in Section 4. We defined three different parameter estimation processes, namely: (1) direct mapping; (2) integration approaches (geostatistical and Bayesian); and (3) joint inversion or fully-coupled hydrogeophysical inversion. Each of these has advantages and limitations, and the decision about which approach to use is a function of the data available, the characterization objective and project budget, and the experience of the interpreter with the different methods. Clearly, the motivation exists to take advantage of the complimentary nature of hydrological and geophysical data and modeling to improve experimental design and interpretation while recognizing that each of these approaches has associated uncertainty. We thus believe that one of the most important developments in hydrogeophysical research in the coming years will arise from data integration schemes that provide a flexible way to couple different hydrological and geophysical data and

model types in a framework that explicitly assesses uncertainty in the final model or model predictions. An important challenge will be the development of methods that disregard models that are inconsistent with our available data and a priori conceptions while retaining a representative subset of models that are consistent with available data. It is expected that joint inversion approaches can provide more significant improvements compared to other approaches, especially when working with time-lapse data and when the hydrological dynamics of the geophysical and hydrological forward responses display strong non-linearities. Although inversion approaches have been developed to meet some of these criteria, for the most part they have been tested in conjunction with specific research projects and are not generally accessible for use by non-specialists or flexible enough to be applied to other problems and datasets. An existing need is thus the development of software that will facilitate the transfer of the state-of-the-art inversion algorithms, which allow joint consideration of geophysical and hydrological measurements and phenomena and that provide meaningful assessments of uncertainty, into practice.

Related to all three key factors in hydrogeophysical studies (high quality geophysical datasets, petrophysics, and integration methods) is the need to better advance our capabilities to improve the characterization of subsurface hydrological parameters and processes at the larger watershed scale. The majority of the hydrogeophysical studies that have focused on quantitative hydrological parameter estimation or model coupling have been performed at the local scale (typically with length scales <10 m), where the disparity in measurement support scale between wellbore (direct) measurements and geophysical measurements is smaller and where stationarity of petrophysical relationships can often be reasonably assumed. Although these studies have

illustrated the power of hydrogeophysical methods for improving the resolution and understanding of subsurface properties or processes at the local scale, they are often still limited in their ability to inform about behavior that may be most relevant at the larger scales where water resources or environmental contaminants are managed. As was described in Section 4, although a handful of case studies have now illustrated the potential that geophysical methods hold for providing quantitative information over large spatial scales, additional effort is needed to continue to advance this area of watershed hydrogeophysics (Robinson et al., 2008). In particular, there is a great need to develop petrophysical models and integration schemes that permit the coupling of different hydrological and geophysical data and model types within a framework that explicitly assesses uncertainty in the final model or model predictions over watershed- or plume-relevant scales.

Acknowledgments

Support for Susan Hubbard was provided by the U.S. Department of Energy, Biological and Environmental Research Program as part of the Oak Ridge Integrated Field Research Center (ORIFRC) project and through DOE Contract DE-AC0205CH11231 to the LBNL Sustainable Systems Scientific Focus Area. We thank Lee Slater and Sebastien Lambot whose constructive reviews helped to substantially improve the text.

7. References

Adepelumi AA, Ako BD, Afolabi O, and Arubayi JB (2005) Delineation of contamination plume around oxidation sewage ponds in southwestern Nigeria. *Environmental Geology* 48: 1137–1146.

Ajo-Franklin JB, Minsley BJ, and Daley TM (2007) Applying compactness constraints to differential traveltime tomography. *Geophysics* 72: R67–R75.

Alumbaugh DL and Newman GA (2000) Image appraisal for 2-D and 3-D electromagnetic inversion. *Geophysics* 65: 1455–1467.

Annan AP (2005) GPR Methods for Hydrogeological Studies. In Y. Rubin and S. Hubbard, eds., *Hydrogeophysics*, Chapter 7, pp 185–214. The Netherlands: Springer.

Archie, GE (1942) The electrical resistivity log as an aid in determining some reservoir parameters. *Transactions of the American Institute of Mining, Metallurgy, and Petroleum Engineering* 146: 54–62.

Atekwana EA., E.A. Atekwana, Werkema DD, Allen JP, Smart LA Duris JW, Cassidy DP, Sauck WA, and Rossbach S (2004). Evidence of microbial enhanced electrical conductivity in hydrocarbon-contaminated sediments, *Geophysics Research Letters*, 31, L2350.

Atekwana EA, Werkema DD, and Atekwana EA (2006) Biogeophysics: The effects of microbial processes on geophysical properties of the shallow subsurface. In: Vereecken H, et al., ed., *Applied Hydrogeophysics*, Chapter 6, pp 161–193. The Netherlands: Springer.

Beres M and Haeni FP (1991) Application of ground-penetrating radar methods in hydrogeological studies. *Ground Water* 29: 375–386.

Beres M, Huggenberger P, Green AG, and Horstmeyer H (1999) Using two- and three-dimensional georadar methods to characterize glaciofluvial architecture. *Sedimentary Geology* 129: 1–24.

Bernabé Y and Revil A (1995) Pore-scale heterogeneity, energy dissipation and the transport properties of rocks. *Geophysical Research Letters* 22: 1529–1532.

Berthold S., Bentley L, and Hayashi M (2004) Integrated hydrogeological and geophysical study of depression-focused groundwater recharge in the Canadian prairies. *Water Resources Research* 40, W06505.

Bigalke J and Grabner EW (1997) The Geobattery model: A contribution to large scale electrochemistry. *Electrochemica Acta* 42: 3443.

Binley A, Cassiani G, Middleton R, and Winship P (2002a) Vadose zone flow model parameterisation using cross-borehole and resistivity imaging. *Journal of Hydrology* 267: 147–159.

Binley A, Cassiani G, Middleton R., and Winship P (2002b) Vadose zone flow model parameterisation using cross-borehole radar and resistivity imaging. *Journal of Hydrology* 267, 147–159.

Binley A. and Kemna A. (2005) DC resistivity and induced polarization methods. In: Y. Rubin and S. Hubbard, eds. *Hydrogeophysics*. Chapter 5, pp 129–156. The Netherlands, Springer.

Binley A, Slater LD, Fukes M, and Cassiani G (2005) Relationship between spectral induced polarization and hydraulic properties of saturated and unsaturated sandstone. *Water Resources Research* 41: W12417.

Birchak JR, Gardner CG, Hipp JE, and Victor JM (1974) High dielectric constant microwave probes for sensing soil moisture. *Proceedings of the IEEE* 62: 93–98.

Blakely RJ (1996) *Potential Theory in Gravity and Magnetic Applications*. UK: Cambridge University Press.

Bolshakov DK, Modin IN, Pervage EV, and Shevnin VA (1997), Separation of anisotropy and inhomogeneity influence by the spectral analysis of azimuthal resistivity diagrams. Paper presented at 3rd EEGS-ES Meeting, Aarhus, Denmark.

Bowling JC, Zheng C, Rodriguez AB, and Harry D (2006) Geophysical constraints on contaminant modeling in a heterogeneous fluvial aquifer. *Journal of Contaminant Hydrology* 85: 72–88.

Brovelli A and Cassiani G (2008) Effective permittivity of porous media: a critical analysis of the complex refractive index model. *Geophysical Prospecting* 56: 715–727.

Brovelli A and Cassiani G (2010) A combination of the Hashin-Shtrikman bounds aimed at modelling electrical conductivity and permittivity of variably saturated porous media. *Geophysical Journal International* 180: 225-237.

Bussian AE (1983) Electrical conductance in a porous medium. *Geophysics* 48: 1258-1268.

Butler J (2005). Hydrogeological methods for estimation of spatial variations in hydraulic conductivity, Chapter 2 in *Hydrogeophysics*, Eds. Y. Rubin and S. Hubbard, Springer,

Börner FD and Schön JH (1991) A relation between the quadrature component of electrical conductivity and the specific surface area of sedimentary rocks. *Log Analyst* 32: 612–613.

Carcione JM, Ursin B, and Nordskag JI, (2007) Cross-property relations between electrical conductivity and the seismic velocity of rocks. *Geophysics* 72: E193–E204.

Cassiani G., Bohm G, Vesnaver A, and Nicholich R (1998) A geostatistical framework for incorporating seismic tomography auxillary data into hydraulic conductivity estimation. *Journal of Hydrology*, 206(1–2): 58–74.

Chapelle FH (2001) *Groundwater Microbiology and Geochemistry*. New York: Wiley.

Chen J, Hubbard S, and Rubin Y (2001) Estimating the hydraulic conductivity at the South Oyster Site from geophysical tomographic data using Bayesian techniques based on the normal linear regression model. *Water Resources Research* 37: 1603–1616.

Chen J., Hubbard S., Peterson J, Williams K, Fienen M, Jardine P, and Watson D (2006), Development of a joint hydrogeophysical inversion approach and application to a contaminated fractured aquifer, Water Resources Research, 42, W06425, doi:10.1029/ 2005WR004694.

Chen J, Hubbard SS, Williams KH, Pride S, Li L, and Slater L (2009) A state-space Bayesian framework for estimating biogeochemical transformations using time-lapse geophysical data. *Water Resources Research* 45, W08420, doi:10.1029/2008WR007698.

Chen J., Hubbard S, Gaines D, Korneev V, Baker G, and Watson D (2010, submitted), Stochastic inversion of seismic refraction data for estimating watershed-scale aquifer geometry: Development and testing within a Contaminated Aquifer. *Water Resources Research*.

Cole KS and Cole RH (1941) Dispersion and absorption in dielectrics, 1. Alternating current characteristics. *Journal of Chemical Physics* 9: 341–351.

Corry CE (1985) Spontaneous polarization associated with porphyry sulfide mineralization. *Geophysics* 50: 1020.

Dafflon B, Irving J, and Holliger K (2009) Simulated-annealing-based conditional simulation for the local-scale characterization of heterogeneous aquifers. *Journal of Applied Geophysics* 68: 60–70.

Davis JL and Annan AP (1989) Ground-penetrating radar for high-resolution mapping of soil and rock stratigraphy. *Geophysical Prospecting* 37: 531–551.

Day-Lewis FD, Harris JM, and Gorelick SM (2002) Time-lapse inversion of crosswell radar data. *Geophysics* 67: 1740–1752.

Day-Lewis FD and Lane JW Jr. (2004) Assessing the resolution-dependent utility of tomograms for geostatistics. *Geophysical Research Letters* 31: L07503.

Day-Lewis FD, Lane JW, and Gorelick SM (2006) Combined interpretation of radar, hydraulic, and tracer data from a fractured-rock aquifer near Mirror Lake, New Hampshire, USA. *Hydrogeology Journal* 14: 1–14.

Day-Lewis FD, Lane, JW Jr., Harris JM, and Gorelick SM (2003) Time-lapse imaging of saline-tracer transport in fractured rock using difference-attenuation radar tomography. *Water Resources Research* 39: 1290.

Day-Lewis FD, Singha K, and Binley A (2005) Applying petrophysical models to radar travel time and electrical resistivity tomograms: Resolution-dependent limitations. *Journal of Geophysical Research* 110: B08206.

D'Ozouville N, Auken E, Sorensen K et al. (2008) Extensive perched aquifer and structural implications revealed by 3D resistivity mapping in a Galapagos volcano. *Earth and Planetary Science Letters* 269: 518–522.

Ernst JR, Maurer H, Green AG, and Holliger K (2007) Full-waveform inversion of crosshole radar data based on 2-D finite-difference time-domain solutions of Maxwell's Equations, *IEEE Transactions on Geoscience and Remote Sensing* 45(9): 2807-2828.

Englert A, Hubbard SS, Williams KH, Li L, and Steefel CI (2009) Feedbacks between hydrological heterogeneity and bioremediation induced biogeochemical transformations. *Environmental Science & Technology* 43(13), 5197–5204.

Everett ME. and Meju MA (2005) Near-surface controlled source electromagnetic induction: Background and recent advances. In Y. Rubin and S. Hubbard, eds., *Hydrogeophysics*, Chapter 6. The Netherlands: Springer.

Falgàs E, Ledo J, Marcuello A, and Queralt P (in review 2009) Monitoring freshwater-seawater interface dynamics with audiomagnetotellurics data. *Near Surface Geophysics*: 391-399.

Farquharson CG (2008) Constructing piecewise-constant models in multidimensional minimum-structure inversions. *Geophysics* 73: K1–K9.

Ferré, T.P.A., A. Binley, J. Geller, E. Hill and T. Illangasekare (2005) Hydrogeophysical methods at the Laboratory Scale, in *Hydrogeophysics,* Eds. Y. Rubin and S. Hubbard, Springer, Netherlands.

Finsterle S (1999) iTOUGH2 User Guide, Lawrence Berkeley National Laboratory LBNL-40040.

Fox RM (1830) On the electromagnetic properties of metalliferous veins in the mines of Cornwall. *Phil. Trans. Royal Soc. London* 130: 399.

Freeze, R.A., and J.A. Cherry (1979) *Groundwater*, Prentice-Hall, New Jersey.

Friedel S (2003) Resolution, stability and efficiency of resistivity tomography estimated from a generalized inverse approach. *Geophysical Journal International* 153: 305–316.

Gallardo LA and Meju MA (2003) Characterization of heterogeneous near-surface materials by joint 2D inversion of dc resistivity and seismic data. *Geophysical Research Letters* 30: 1658.

Gallardo LA and Meju MA (2004) Joint two-dimensional DC resistivity and seismic travel time inversion with cross-gradient constraints. *Journal of Geophysical Research* 109*:* B03311.

Gallardo LA and Meju MA (2007) Joint two-dimensional cross-gradient imaging of magnetotelluric and seismic traveltime data for structural and lithological classification. *Geophysical Journal International* 169: 1261–1271.

Gelhar (1993), *Stochastic Subsurface Hydrology*. New York: Prentice Hall.

Ghorbani A, Camerlynck C, Florsch N, Cosenza P, and Revil A (2007) Bayesian inference of the Cole–Cole parameters from time- and frequency-domain induced polarization. *Geophysical Prospecting* 55: 589–605.

Gloaguen E., Chouteau M, Marcotte D, and Chapuis R (2001) Estimation of hydraulic conductivity of an unconfined aquifer using cokriging of GPR and hydrostratigraphic data. *Journal of Applied Geophysics* 47(2): 135–152.

Goldie M (2002) Self-potentials associated with the Yanacocha high-sulfidation gold deposit in Peru. *Geophysics* 67: 684–689.

Golub GH, and van Loan CF (1996) *Matrix Computations*. 3rd ed., Baltimore, MD: Johns Hopkins Press.

Grasmueck M (1996) 3-D ground-penetrating radar applied to fracture imaging in gneiss. *Geophysics* 61: 1050–1064.

Greaves RJ, Lesmes DP, Lee JM, and Toksov MN (1996) Velocity variations and water content estimated from multi-offset, ground-penetrating radar. *Geophysics* 61, 683–695.

Grote K, Hubbard SS and Rubin Y (2003) Field-scale estimation of volumetric water content using GPR ground wave techniques. *Water Resources Research* 39: 1321–1333.

Guéguen Y and Palciauskas V (1994) *Introduction to the Physics of Rocks*. Princeton, New Jersey: Princeton University Press.

Günther T, Rücker C, and Spitzer K (2006) Three-dimensional modelling and inversion of dc resistivity data incorporating topography – II. Inversion. *Geophysical Journal International* 166: 506-517.

Hashin Z and Shtrikman S (1962) A variational approach to the theory of the effective magnetic permeability of multiphase materials. *Journal of Applied Physics* 33: 3125–3131.

Hastings WK (1970) Monte Carlo sampling methods using Markov chains and their applications. *Biometrika* 57: 97–109.

Hertrich M., (2008) Imaging of groundwater with nuclear magnetic resonance. *Progress in Nuclear Magnetic Resonance Spectroscopy* 53: 227–248.

Hill M. (2006) The practical use of simplicity in developing groundwater models. *Ground Water* 44 (6): 775–781.

Hinze WJ (1990) The role of gravity and magnetic methods in engineering and environmental studies. In: Ward S, ed., *Geotechnical and Environmental Geophysics Vol. 1: Review and Tutorial, SEG Investigations in Geophysics No. 5*, pp 75–126.

Hsieh PA and Shapiro AM (1996) Hydraulic characteristics of fractured bedrock underlying the FSE well field at the Mirror Lake Site, Grafton Country, New Hampshire. In: D. W. Morganwalp DW and Aronson DA, eds., U.S. Geological Survey Toxic Substances Hydrology Program: Proceedings of the Technical Meeting, Colorado Springs, Colorado,

September 20–24, 1993, *U. S. Geological Survey Water Resources Investigative Rep*ort 94-4015, 1: 127–130.

Hördt A, Blaschlek R, Kemna A, and Zisser N (2007) Hydraulic conductivity estimation from induced polarisation data at the field scale—The Krauthausen case history. *Journal of Applied Geophysics* 62: 33–46.

Huisman S, Hubbard SS, Redman D, Annan P (2003) Monitoring soil water content with ground-penetrating radar: A review. *Vadose Zone Journal* 2: 476–491.

Hubbard, S. and Y. Rubin (1997) Ground Penetrating Radar Assisted Saturation and Permeability Estimation in Bimodal Systems, *Water Resources Research*, 33(5), 971-990.

Hubbard S, Peterson JE, Majer EL, Zawislanski PT, Roberts J, Williams KH, and Wobber F (1997) Estimation of permeable pathways and water content using tomographic radar data. *The Leading Edge of Exploration* 16(11): 1623–1628.

Hubbard S**,** Chen J, Peterson J, Majer E, Williams K, Swift D, Mailliox B, and Rubin Y (2001), Hydrogeological characterization of the DOE Bacterial Transport Site in Oyster, Virginia, using geophysical data. *Water Resources Research* 37(10): 2431–2456.

Hubbard, SS., Williams K, Conrad M, Faybishenko B, Peterson J, Chen J, Long P, and Hazen TC (2008) Geophysical monitoring of hydrological and biogeochemical transformations associated with Cr(VI) biostimulation. *Environmental Science and Technology*, DOI 10.1021/es071702s.

Hubbard S., Lunt I, Grote K, and Rubin Y (2006) Vineyard soil water content: mapping small scale variability using ground penetrating radar. In: Macqueen RW and Meinert LD (eds.) *Fine Wine and Terroir—The Geoscience Perspective*. Geoscience Canada Reprint Series

Number 9, Geological Association of Canada, St. John's, Newfoundland, ISBN 1-897095-21-X; ISSN 0821-381X.

Huisman JA, Rings J, Vrugt JA, Sorg J, and Vereecken H (2010) Hydraulic properties of a model dike from coupled Bayesian and multi-criteria hydrogeophysical inversion. *Journal of Hydrology* 380: 62-73.

Hyndman DW and Gorelick SM (1996) Estimating lithologic and transport properties in three dimensions using seismic and tracer data: The Kesterson aquifer. *Water Resources Research* 32(9): 2659–2670.

Hyndman, DW, Harris JM, and Gorelick SM**.** (2000), Inferring the relationship between seismic slowness and hydraulic conductivity in heterogeneous aquifers. *Water Resources Research* 36(8): 2121–2132.

Irving J, Knight R, and Holliger K (in press 2009) Estimation of the lateral correlation structure of subsurface water content from surface-based ground-penetrating radar reflection images. *Water Resources Research*.

Jackson D (1976) Most squares inversion. *Journal of Geophysical Research* 81: 1027–1030.

Johnson DL, Koeplik J, and Schwartz LM (1986) New pore-size parameter characterizing transport in porous media. *Physical Review Letters* 57: 2564-2567.

Juhlin C and Stephens MB (2006) Gently dipping fracture zones in Paleoproterozoic metagranite, Sweden: Evidence from reflection seismic and cored borehole data and implications for the disposal of nuclear waste. *Journal of Geophysical Research* 111: B09302.

Kalscheuer T, and Pedersen LB (2007) A non-linear truncated SVD variance and resolution analysis of two-dimensional magnetotelluric models. *Geophysical Journal International* 169: 435–447.

Keller GV (1987) Rock and mineral properties. In: Nabighian MN (ed) *Electromagnetic Methods in Applied Geophysics, Vol. 1–Theory*. SEG, *Investigations in Geophysics* 3: 13–51.

Kemna A, Binley A, Ramirez A, and Daily W (2000) Complex resistivity tomography for environmental applications. *Chemical Engineering Journal* 77: 11–18.

Keys SW (1989) *Borehole Geophysics Applied to Ground-Water Investigations*. Dublin, OH: National Water Well Association.

Knight R (1991) Hysteresis in the electrical resistivity of partially saturated sandstone. *Geophysics* 56: 2139–2147.

Kobr M., Mares S, and Paillet F (2005), Geophysical well logging: borehole geophysics for hydrogeological studies: principles and applications. In: Rubin Y and Hubbard S (eds.) *Hydrogeophysics*, Chapter 10, pp 291–332. The Netherlands: Springer.

Koch K, Wenninger J, Uhlenbrook S, and Bonell M (2009) Joint interpretation of hydrological and geophysical data: Electrical resistivity tomography results from a process hydrological research site in the Black Forest Mountains, Germany. *Hydrological Processes* 23: 1501–1513.

Kowalsky MB, Finsterle SA, and Rubin Y. (2004), Estimating flow parameter distributions using ground-penetrating radar and hydrological measurements during transient flow in the vadose zone. *Advances in Water Resources* 27(6): 583–599.

Kowalsky MB, Finsterle S, Peterson J, et al. (2005) Estimation of field-scale soil hydraulic and dielectric parameters through joint inversion of GPR and hydrological data. *Water Resources Research* 41: W11425.

Kowalsky MB, Chen J, and Hubbard S (2006) Joint inversion of geophysical and hydrological data for improved subsurface characterization. *The Leading Edge* 26(5): Society of Exploration Geophysicists.

Krause P, Naujoks M, Fink M and Kroner C (2009) The impact of soil moisture changes on gravity residuals obtained with a superconducting gravimeter. *Journal of Hydrology* 373: 151-163.

LaBrecque DJ and Yang X (2001) Difference inversion of ERT data: A fast inversion method for 3-D in situ monitoring. *JEEG* 6: 83–89.

Lambot S, Slob EC, van den Bosch I, Stockbroeckx B, and Vanclooster M (2004a) Modeling of ground penetrating radar for accurate characterization of subsurface electric properties. *IEEE Transactions on Geoscience and Remote Sensing* 42: 2555-2568.

Lambot, S, Rhebergen J, van den Bosch I, Slob EC, and Vanclooster M (2004b) Measuring the soil water content profile of a sandy soil with an off-ground monostatic ground penetrating radar. *Vadose Zone Journal* 3: 1063-1071.

Lambot S, Binley A, Slob E, and Hubbard S (2008) Ground penetrating radar in hydrogeophysics. *Vadose Zone Journal* 7: 137–139, doi: 10.2136/vzj2007.0180.

Lambot S, Weihermüller L, Huisman JA, Vereecken H, Vanclooster M, and Slob EC (2006) Analysis of air-launched ground-penetrating radar techniques to measure the soil surface water content. *Water Resources Research* 42: W11403, doi:10.1029/2006WR005097.

Lambot, S, Slob E, Rheberger J, Lopera O, Jadoon KZ, and Vereecken H (2009). Remote estimation of the hydraulic properties of a sand using full-waveform integrated hydrogeophysical inversion of time-lapse, off-ground GPR data. *Vadose Zone Journal* 8: 743-754.

Lane JW, Jr., Haeni FP, and Watson WM (1995) Use of square-array direct-current resistivity method to detect fractures in crystalline bedrock in New Hampshire. *Ground Water* 33: 476–485.

Leroy P and Revil A (in press 2009) A mechanistic model for the spectral induced polarization of clay materials. *Journal of Geophysical Research*, doi:10.1029/2008JB006114.

Leroy P and Revil A (2004) A triple-layer model of the surface electrochemical properties of clay minerals. *Journal of Colloid and Interface Science* 270: 371–380.

Leroy P, Revil A, Kemna A, Cosenza P, and Ghorbani A (2008) Complex conductivity of water-saturated packs of glass beads. *Journal of Colloid and Interface Sciences* 321: 103–117.

Lesmes DP, and Friedman SP (2005) Relationships between the electrical and hydrogeological properties of rocks and soils. In Rubin Y and Hubbard SS (eds.) *Hydrogeophysics*, pp 87–128. The Netherlands: Springer.

Li L, Steefel CI, Williams KH, Wilkins MJ, and Hubbard SS (2009) Mineral transformation and biomass accumulation during uranium bioremediation at Rifle, Colorado. *Environmental Science and Technology* 43(14): 5429–5435.

Lien M and Mannseth T (2008) Sensitivity study of marine CSEM data for reservoir production monitoring. *Geophysics* 73: F151–F163.

Linde N (2009) A comment on “Characterization of multiphase coupling using a bundle of capillary tubes model” by M. D. Jackson [Journal of Geophysical Research, 113, B04201]. *Journal of Geophysical Research* 114: *B06209*.

Linde N, Binley A, Tryggvason A, Pedersen LB, and Revil A (2006a) Improved hydrogeophysical characterization using joint inversion of cross-hole electrical resistance and ground-penetrating radar traveltime data. *Water Resources Research* 42: W12404.

Linde N, Chen J, Kowalsky MB, and Hubbard S (2006b) Hydrogeophysical parameter estimation approaches for field scale characterization. In: Vereecken et al. (eds) *Applied Hydrogeophysics,* Chapter 2, pp. 9–44. The Netherlands: Springer.

Linde N, Finsterle S, and Hubbard S (2006c) Inversion of tracer test data using tomographic constraints. *Water Resources Research* 42: W04410.

Linde N, Jougnot D, Revil A, et al. (2007) Streaming current generation in two-phase flow conditions. *Geophysical Research Letters* 34: L03306.

Linde N and Pedersen LB (2004) Evidence of electrical anisotropy in limestone formations using the RMT technique. *Geophysics* 69: 909–916.

Linde N and Revil A (2007) Inverting self-potential data for redox potentials of contaminant plumes. *Geophysical Research Letters* 34: L14302, doi: 10.1029/2007GL030084.

Linde N, Tryggvason A, Peterson J, and Hubbard S (2008) Joint inversion of crosshole radar and seismic traveltimes. *Geophysics* 73: G29–G37.

Lunt IA, Bridge JS, and Tye RS (2004) A quantitative, three-dimensional depositional model of gravelly braided rivers. *Sedimentology* 51: 377–414.

Lunt IA, Hubbard SS, and Rubin Y (2005). Soil moisture content estimation using ground-penetrating radar reflection data. *Journal of Hydrology* 307: 254–269.

Mair JA, and Green AG (1981) High-resolution seismic-reflection profiles reveal fracture-zones within a homogeneous granite batholith. *Nature* 294: 439–442.

Maurer H, Holliger K, and Boerner DE (1998) Stochastic regularization: Smoothness or similarity? *Geophysical Research Letters* 25: 2889–2892.

Mavko G, Mukerji T, and Dvorkin J (1998) *The Rock Physics Handbook*. UK: Cambridge University Press.

McLaughlin D and Townley LR (1996) A reassessment of the groundwater inverse problem. *Water Resources Research* 32: 1131–1161.

Menke W (1984) *Geophysical data analysis—Discrete inverse theory*. New York: Academic Press.

Minsley BJ, Sogade J, and Morgan FD (2007) Three-dimensional source inversion of self-potential data. *Journal of Geophysical Research* 112: B02202.

Molz, F., G.K. Boman, S.C. Young, W.R. Waldrop (1994), Borehole flowmeters: Field applications and data analysis, *Journal of Hydrology*, 163: 347-371.

Mosegaard K, and Tarantola A (1995) Monte-Carlo sampling of solutions to inverse problems. *Journal of Geophysical Research* 100: 12431–12447.

Moysey S Singha K, and Knight R (2005) A framework for inferring field-scale rock physics relationships through numerical simulation. *Geophysical Research Letters* 32: L08304.

Naudet V, Revil A, Bottero JY, and Begassat P (2003) Relationship between self-potential (SP) signals and redox conditions in contaminated groundwater. *Geophysical Research Letters* 30: 2091.

Naudet V, Revil A, Rizzo E, Bottero JY, and Begassat P (2004) Groundwater redox conditions and conductivity in a contaminant plume from geoelectrical investigations. *Hydrology and Earth Systems Sciences* 8: 8–22.

Nguyen F, Kemna A, Antonsson A, et al. (2009), Characterization of seawater intrusion using 2D electrical imaging, *Near Surface Geophysics*: 377-390.

NRC (1996) *Rock Fractures and Fluid Flow*. Washington D.C.: National Academy Press.

Ogilvy RD, Meldrum PI, Kuras I, et al. (2009), Automated monitoring of coastal aquifers with electrical resistivity tomography, *Near Surface Geophysics*: 367-375.

Oldenburg DW and Li Y (1999) Estimating the depth of investigation in dc resistivity and IP surveys. *Geophysics* 64: 403–416.

Olsson O, Falk L, Forslund O, Lundmark L, and Sandberg E (1992) Borehole radar applied to the characterization of hydraulically conductive fracture zones in crystalline rock. *Geophysical Prospecting* 40: 109–142.

Paine, JG (2003) Determining salinization extent, identifying salinity sources, and estimating chloride mass using surface, borehole, and airborne electromagnetic induction methods. *Water Resources Research* 39(3): 3-1–3-10.

Parker RL (1994) *Geophysical Inverse Theory*. Princeton, N.J.: Princeton University Press.

Pedersen LB, Qian W, Dynesius L, and Zhang P (1994) An airborne tensor VLF system–From concept to realization. *Geophysical Prospecting* 42: 863–883.

Poldini E (1938), Geophysical exploration by spontaneous polarization methods. *Mining Mag., London*, 59: 278–282.

Pollock DA and Cirpka OA (2008) Temporal moments in geoelectrical monitoring of salt tracer experiments. *Water Resources Research* 44: W12416.

Pride S (1994) Governing equations for the coupled electromagnetics and acoustics of porous media. *Physical Review B* 50: 15678–15696.

Purvance D and Andricevic R (2000) On the electrical-hydraulic conductivity correlation in aquifers. *Water Resources Research* 36: 2905–2913.

Revil A, and Cathles LM (1999) Permeability of shaly sands. *Water Resources Research* 35: 651–662.

Revil A, Cathles LM, Losh S, and Nunn JA (1998) Electrical conductivity in shaly sands with geophysical applications. *Journal of Geophysical Research* 103: 23'925–23'936.

Revil A and Glover PWJ (1998) Nature of surface electrical conductivity in natural sands, sandstones, and clays. *Geophysical Research Letters* 25: 691–694.

Revil A and Glover PWJ (1997) Theory of ionic-surface electrical conduction in porous media. *Physical Review B* 55: 1757–1773.

Revil A and Leroy P (2004) Constitutive equations for ionic transport in porous shale's. *Journal of Geophysical Research* 109: B03208.

Revil A., Naudet V, Nouzaret J, and Pessel M (2003) Principles of electrography applied to self-potential electrokinetic sources and hydrogeological applications. *Water Resources Research* 39(5), 1114.

Revil A and Linde N (2006) Chemico-electromechanical coupling in microporous media. *Journal of Colloid and Interface Sciences* 302: 682–694.

Ritzi RW, Dai ZX, Dominic DF, and Rubin YN (2004) Spatial correlation of permeability in cross-stratified sediment with hierarchical architecture. *Water Resources Research* 40: W03513.

Robinson DA, Binley A, Crook N, et al. (2008), Advancing process-based watershed hydrological research using near-surface geophysics: a vision for, and review of, electrical and magnetic geophysical methods. Hydrological Processes 22: 3604-3635.

Rubin Y and Hubbard S (2005), *Hydrogeophysics*, Water and Science Technology Library, vol 50. The Netherlands: Springer.

Rucker DF and Fink JB (2007) Inorganic plume delineation using surface high resolution electrical resistivity at the BC Cribs and Trenches Site, Hanford. *Vadose Zone Journal* 6: 946–958.

Sassen DS and Everett ME (2009) 3D polarimetric GPR coherency attributes and full-waveform inversion of transmission data for characterizing fractured rock. *Geophysics* 74: doi:10.1190/1.3103253

Sato M and Mooney HM (1960) The electrochemical mechanism of sulfide self-potentials. *Geophysics* 25: 226–249.

Saunders JH, Herwanger JV, Pain CC, Worthington MH, and de Oliveira CRE (2005) Constrained resistivity inversion using seismic data. *Geophysical Journal International* 160: 785–796.

Scheibe TD and Chien YJ (2003) An evaluation of conditioning data for solute transport prediction. *Ground Water* 41(2): 128–141.

Scheibe, T., Y. Fang, C.J. Murray, E. E. Roden, J. Chen, Y. Chien, S.C. Brooks, S. S. Hubbard (2006) Transport and biogeochemical reactions of metals in a and chemically heterogeneous aquifer, *Geosphere*, 2(4), doi: 10.1130/GES00029.1.

Scott JBT and Barker RD (2003) Determining pore-throat size in Permo-Triassic sandstones from low-frequency electrical spectroscopy. *Geophysical Research Letters 30*: 1450.

Schwarz LM, Sen PN, and Johnson DL (1989) Influence of rough surfaces on electrolytic conduction in porous media. *Physical Review B* 40: 2450–2458.

Schön JH (1996) *Physical Properties of Rocks—Fundamentals and Principles of Petrophysics*. Amsterdam, The Netherlands: Elsevier.

Sen PS, Goode PA, and Sibbit A (1988) Electrical conduction in clay bearing sandstones at low and high salinities. *Journal of Applied Geophysics* 63: 4832–4840.

Sen PN, Scala C, and Cohen MH (1981) A self-similar model for sedimentary rocks with application to the dielectric constant of fused glass beads. *Geophysics* 46: 781–795.

Shokri N, Lehmann P, and Or D (2009) Characteristics of evaporation from partially wettable porous media. *Water Resources Research* 45: W02415.

Sill WR (1983) Self-potential modeling from primary flows. *Geophysics* 48: 76–86.

Singha K, and Gorelick SM (2005) Saline tracer visualized with three-dimensional electrical resistivity tomography: Field-scale spatial moment analysis. *Water Resources Research* 41: W05023.

Slater L (2007) Near surface electrical characterization of hydraulic conductivity: from petrophysical properties to aquifer geometries—A review. *Surveys in Geophysics* 28: 167–197.

Slater L, Atekwana E, and Brantley S, et al. (2009) Exploring the geophysical signatures of microbial processes, *Eos Transactions AGU* 90: 83.

Slater L and Lesmes DP (2002) Electrical-hydraulic relationships observed for unconsolidated sediments. *Water Resources Research* 38: 1213.

Slater, L., D. Ntarlagiannis, and D. Wishard, (2006) On the relationship between induced polarization and surface area in metal-sand and clay-sand mixtures, *Geophysics*, 71: A1-A5.

Slater L., Ntarlagniannis D, Personna Y, and Hubbard S (2007) Pore-scale spectral induced polarization (SIP) signatures associated with FeS biomineral transformations. *Geophysical Research Letters* 34: L21404, doi:10.1029/2007GL031840.

Sørensen KI and Auken E (2004) SkyTEM—A new high-resolution helicopter transient electromagnetic system. *Exploration Geophysics* 35: 191–199.

Spillmann T, Maurer H, Willenberg H, et al. (2007) Characterization of an unstable rock mass based on borehole logs and diverse borehole radar data. *Journal of Applied Geophysics* 61: 16–38.

Steeples D. (2005). Shallow seismic methods. In: Rubin Y and Hubbard S (eds.) *Hydrogeophysics*, Chapter 7, pp 215–252. The Netherlands: Springer.

Stummer P, Maurer H, and Green AG (2004), Experimental design: Electrical resistivity data sets that provide optimum subsurface information. *Geophysics* 69: 120–139.

Styles P, McGrath R, Thomas E, and Cassidy NJ (2005) The use of microgravity for cavity characterization in karstic terrains. *Quarterly Journal of Engineering Geology and Hydrogeology* 38(2): 155-169.

Suski B, Revil A, Titov K, Konosavsky P, Voltz M, Dagès C and Huttel O (2006) Monitoring of an infiltration experiment using the self-potential method. *Water Resources Research* 42: W08418.

Talley J, Baker GS, Becker MW, and Beyrle N (2005) Four dimensional mapping of tracer channelization in subhorizontal bedrock fractures using surface ground penetrating radar. *Geophysical Research Letters* 32: L04401.

Tarantola A (2005) *Inverse Problem Theory and Methods for Model Parameter Estimation*. Philadelphia, PA: Society for Industrial and Applied Mathematics (SIAM).

Taylor RW and Fleming AH (1988) Characterizing jointed systems by azimuthal resistivity techniques. *Ground Water* 26: 464–474.

Telford WM, Geldart LP, and Sheriff RE (1990), *Applied Geophysics*. UK: Cambridge University Press.

Titov KV., Levitski A, Knoosavski PK, Tarasov AV, Ilyin YT and Bues MA, (2005) Combined application of surface geoelectrical methods for groundwater-flow modeling: A case history. *Geophysics* 70(5): H21–H31.

Topp GC, Davis JL, and Annan AP (1980) Electromagnetic determination of soil water content: Measurements in coaxial transmission lines. *Water Resources Research* 16: 574–582.

Tsoflias GP and Becker MW (2008) Ground-penetrating-radar response to fracture-fluid salinity: Why lower frequencies are favorable for resolving salinity changes. *Geophysics* 73: J25–J30.

Tsoflias GP, Halihan T, and Sharp JM, Jr. (2001) Monitoring pumping test response in a fractured aquifer using ground-penetrating radar. *Water Resources Research* 37: 1221–1229.

van Overmeeren RA (1998) Radar facies of unconsolidated sediments in The Netherlands: A radar stratigraphy interpretation method for hydrogeology. *Journal of Applied Geophysics* 40: 1–18.

Vereecken H, Huisman JA, Bogena H, Vanderborght J, Vrugt JA and Hopmans JW (2008). On the value of soil moisture measurements in vadose zone hydrology: a review. *Water Resources Research* 44, W00D06.

Vereecken H, Binley A, Gassiani G, Revil A, and Titov K (2006) *Applied Hydrogeophysics*, NATO Science Series, Earth and Environmental Science Vol. 71, Springer, Netherlands.

Viezzoli A, Christiansen AV, Auken E, and Sørensen K (2008) Quasi-3D modeling of airborne TEM data by spatially constrained inversion. *Geophysics* 73: F105–F113.

Vrugt JA, ter Braak CJF, Diks CGH, et al. (2009) Accelerating Markov Chain Monte Carlo simulation by differential evolution with self-adaptive randomized subspace sampling. *International Journal of Nonlinear Sciences and Numerical Simulation* 10: 273–290.

Watson KA and Barker RD (1999) Differentiating anisotropy and lateral effects using azimuthal resistivity offset Wenner soundings. *Geophysics* 64: 739–745.

Watson DB, Doll WE, Gamey TJ, Sheehan JR, and Jardine PM (2005) Plume and lithologic profiling with surface resistivity and seismic tomography. *Ground Water* 43(2):169–177.

Waxman MH and Smits LJM (1968) Electrical conductivities in oil-bearing shaly sands. *Transactions AIME* 243: 107–122.

Wilkinson PB, Meldrum PI, Chambers JE, Kuras O and Ogilvy R (2006), Improved strategies for the automatic selection of optimized sets of electrical resistivity tomography measurement configurations. *Geophysical Journal International* 167: 1119-1126.

Williams KH., Kemna A, Wilkins M, Druhan J, Arntzen E, N'Guessan L, Long PE, Hubbard SS, and Banfield JF (2009) Geophysical monitoring of microbial activity during stimulated subsurface bioremediation. *Environmental Science and Technology*, DOI 10.1021/es900855j.

Williams KH, Ntarlagiannis D, Slater LD, Dohnalkova A, Hubbard SS, and Banfield JF (2005) Geophysical imaging of stimulated microbial biomineralization. *Environmental Science and Technology* 39(19): 7592–7600.

Wishart DN, Slater LD, and Gates A (2008) Fracture anisotropy characterization in crystalline bedrock using field-scale azimuthal self potential gradient. *Journal of Hydrology* 358: 35–45.

Wishart DN, Slater LD, and Gates AE (2006) Self potential improves characterization of hydraulically-active fractures from azimuthal geoelectrical measurements. *Geophysical Research Letters* 33: L17314.

Yaramanci U, Kemna A, and Vereecken H (2005) Emerging technologies in hydrogeophysics. In: Rubin Y and Hubbard S (eds.) *Hydrogeophysics*, Chapter 16. The Netherlands: Springer.

Zhdanov MS (2009) New advances in regularized inversion of gravity and electromagnetic data. *Geophysical Prospecting* 57: 463–478.

Zonge KL and Hughes LJ (1991) Controlled source audio-frequency magnetotellurics. In: Nabighian MN (ed.) *Electromagnetic Methods in Applied Geophysics*, *Vol. 2—Applications*. pp 713–810. Tulsa, OK: Society of Exploration Geophysicists.